BENZOSELENADIAZOLE, QUINOXALINE AND THIENOTHIOPHENE BASED MONOMERS; ELECTROCHEMICAL AND SPECTROELECTROCHEMICAL PROPERTIES

A THESIS SUBMITTED TO
THE GRADUATE SCHOOL OF NATURAL AND APPLIED SCIENCES
OF
MIDDLE EAST TECHNICAL UNIVERSITY

BY
SİNEM TOKSABAY

IN PARTIAL FULFILLMENT OF THE REQUIREMENTS
FOR
THE DEGREE OF MASTER OF SCIENCE
IN
CHEMISTRY

APRIL 2014

Approval of the thesis:

BENZOSELENADIAZOLE, QUINOXALINE AND THIENOTHIOPHENE BASED MONOMERS; ELECTROCHEMICAL AND SPECTROELECTROCHEMICAL PROPERTIES

submitted by **SİNEM TOKSABAY** in partial fulfillment of the requirements for the degree of **Master of Science in Chemistry Department, Middle East Technical University** by,

Prof. Dr. Canan Özgen _____
Dean, Graduate School of **Natural and Applied Sciences**

Prof. Dr. İlker Özkan _____
Head of Department, **Chemistry**

Prof. Dr. Levent Toppare _____
Supervisor, **Chemistry Dept., METU**

Examining Committee Members:

Assoc. Prof. Dr. YaseminUdum
Institute of Science and Technology, _____
Department of Advanced Technologies,
Gazi University

Assoc. Prof. Dr. Ali Çırpan _____
Chemistry Dept., METU

Prof. Dr. Levent Toppare _____
Chemistry Dept., METU

Assist. Prof. Dr. İrem Erel Göktepe _____
Chemistry Dept., METU

Dr. Görkem Günbaş _____
Chemistry Dept., METU

Date: 22.04.2014

I hereby declare that all information in this document has been obtained and presented in accordance with academic rules and ethical conduct. I also declare that, as required by these rules and conduct, I have fully cited and referenced all material and results that are not original to this work.

Name, Last name: Sinem TOKSABAY

Signature:

ABSTRACT

BENZOSELENADIAZOLE, QUINOXALINE AND THIENOTHIOPHENE BASED MONOMERS; ELECTROCHEMICAL AND SPECTROELECTROCHEMICAL PROPERTIES

Toksabay, Sinem

M. Sc., Department of Chemistry

Supervisor: Prof. Dr. Levent Toppare

April 2014, 70 pages

A new age had been started in macromolecular science with the invention of conducting polymers and they have gained considerable attention due to the their advantages of low cost, high molecular weight, easy fabrication and compability with flexible substrates. It was found that they can be used in many fields, such as organic light emitting diodes, electrochromic materials, organic solar cellsr, organic field effect transistors and sensors . Donor-acceptor phenomenon, which provide the band gap altenation due to the electron rich and electron poor building blocks in the polymer main chain, is one of the most favored technique for designing organic conducting polymers. Through regulating the contribution of intramolecular charge transfer (ICT) , the absorption spectra and energy levels of D-A type polymers can be tuned. Benzoselenadiazole, quinoxaline and thienothiophene are units commonly utilized in conducting polymers due to their suitable electrochemical properties. However there are no reports in the literature on polymers containing both moieties.

With this motivation, we designed and synthesized such a monomer. In this study, two novel benzoselenadiazole, quinoxaline and thienothiophene based monomers; 4-(3a,6a-dihydrothieno[3,2-b]thiophen-2-yl)-7-(thieno[3,2-b]thiophen yl)benzo[c][1,2,5]selenadiazole **(BSeTT)** and 2,3-bis(3,4-bis(decyloxy)phenyl)-5,8-dibromo-2,3-dihydroquinoxaline **(QTT)** were synthesized via Stille Coupling and polymerized electrochemically. These polymers were then characterized in terms of their spectroelectrochemical and electrochemical properties by cyclic voltammetry and UV-Vis-NIR spectroscopy. Spectroelectrochemistry analysis of **P(BSeTT)** revealed an electronic transition at 525 nm corresponding to π – π* transition with a band gap of 0.93 eV whereas P(QTT) revealed an electronic transition at 440 and 600 nm corresponding to π- π* transition with a band gap of 1.30 eV. Investigation of electrochromic properties showed that **P(BSeTT)** has gray color and **P(QTT)** switches between green and gray. Switching times of the polymers were evaluated by a kinetic study upon measuring the percent transmittance (%T) at the maximum contrast point.

Keywords: **C**onducting polymer, electrochemically polymerization, thienothiophene, donor-acceptor theory.

ÖZ

BENZOSELENADİYAZOL, KİNOKSALİN, TİYONOTİYOFEN TEMELLİ MONOMERLER; ELEKTROKİMYASAL VE SPEKTROELEKTROKİMYASAL ÖZELLİKLERİ

Toksabay, Sinem

Yüksek Lisans, Kimya Bölümü

Tez Yöneticisi: Prof. Dr. Levent Toppare

Nisan 2014, 70 sayfa

İletken polimerlerin keşfiyle makromoleküler biliminde yeni bir çağ başladı ve düşük maaliyet, yüksek ağırlık, üretim kolaylığı, elastik yüzeylere uygulanabilirlik gibi özelliklerinden dolayı büyük bir ilgi kazanmıştır. İletken polimerlerin organik ışık yayan diyotlar, organik güneş gözeleri elektrokromik materyaller, organik alan etkili transistörler ve sensörlerde kullanılabileceği bulunmuştur. Polimer ana zincirindeki elektronca zengin ve fakir yapı taşları sayesinde bant aralığı değişimini sağlayabilen donor-akseptör olgusu, organik iletken polimerlerin tasarlanmasında en çok tercih edilen tekniklerden biridir. Moleküller arası yük transfer katkısının ayarlanmasıyla D-A tipi polimerlerin soğurum spektrumları ve enerji seviyeleri ayarlanabilir. Benzoselenadiyazol, kinoksalin ve tiyonotiyofen elektrokimyasal özellikleri bakımından iletken polimerlerde tercih edilen yapılardandır. Literatürde bu yapıları

bir arada bulunduran bir çalışma bulunmamktadır. Bu motivasyon ile bu grupları içeren monomerleri tasarladık ve sentezlemeye karar verdik. Bu çalışmada yeni benzoselenadiyazol, kinoksalin ve tiyonotiyofen bulunduran monomerler Stille kenetlenme reaksiyonu ile sentezlendi ve elektrokimyasal olarak polimerleştirildi. bu polimerlerin spektroelektrokimyasal ve elektrokimyasal özellikleri döngüsel voltametri ve UV-Vis-NIR spektrometresi ile karakteriz edildi. Spectroelektrokimyasal analizler **P(BSeTT)**'nin spektroelektrokimyasal analizi sonucu π-π* geçişi 525 nm'de gözlenmiş ve bant aralığı 0.93 eV olarakhesaplanmıştır, öte yandan **P(QTT)**'nin λmax ve Eg değerleri sırasıyla nm ve 1.30 eV bulunmuştur. Elektrokromik çalışmalar sonucunda **P(BSeTT)**'nin gri, **P(QTT)**'nin yeşil ve gri arasında değiştiği gözlemlenmiştir. Renklerin değişim hızları kinetik çalışma ile yüzde transmitansın en yüksek kontrast farkında ölçülmüştür. (%T)

Anahtar kelimer: İletken polimer, elektrokimyasal polimerleşme, tiyonotiyofen, donör-akseptör teori.

To My Precious Family

ACKNOWLEDGMENTS

I would like to express my deepest gratitude to my thesis supervisor Prof. Dr. Levent Toppare for his endless guidance, help and patience throughout my study. I am so grateful to him for giving me the chance to work with him. It has been an honor for me to be his graduate student.

I would like to express my appreciation to Naime A. Ünlü for her brilliant ideas, endless help and support during my thesis study. I cannot do anything without her motivation and help.

I would like to thank to Şerife Ö. Hacıoğlu for teaching organic synthesis and characterization of polymers.

Thanks go to all Toppare and Çırpan Research Group members for their cooperation.

I would like to give my special thanks Sinem Çokoğlu, Işılay Sheridan, Selcan Başoğlu Neşe Çevirim and Ela Kılıç for being with me and supporting me all the time whenever I need. They showed me that the distance means nothing in real friendships, I am a very lucky person to be their sister.

I owe great thanks Nilay Koyuncu, Zehra Oluz and Betül Eymur for making my new life a lot easier with their friendship, support and all the fun times we had in the house.

I owe special thanks to Seza Göker, Gönül Hızalan Özsoy, Melis Kesik, Merve İleri, Ebru Işık and Çağla İstanbulluoğlu for their endless support, real friendship and funny gossip times. They provided me great with a great working environment. I wish we could make this before.

Words fail to express my eternal gratitude to my family for believing in me and for their endless support. I am the luckiest and happiest person in the world being their daughter and sister. It won't be possible for me to succeed anything without them.

TABLE OF CONTENTS

LIST OF TABLES

LIST OF FIGURES

FIGURES

LIST OF ABBREVATIONS

A	Acceptor
ACN	Acetonitrile
Ag	Silver
CB	Conduction Band
CE	Counter Electrode
$CHCl_3$	Chloroform
CP	Conducting Polymer
CV	Cyclic Voltammetry
DCM	Dichloromethane
DMF	Dimethylformamide
D	Donor
E_g	Band gap
EDOT	3,4-Ethylenedioxythiophene
EtOH	Ethanol
Fc	Ferrocene
FTIR	Fourier Transform Infrared Spectroscopy
HOMO	Highest Occupied Molecular Orbital
ITO	Indium Tin Oxide
NHE	Normal Heydrogen Electrode
NIR	Near Infrared
NMR	Nuclear Magnetic Resonance Spectrometer
NaOAc	Sodium acetate
Pt	Platinum
PAc	Polyacetylene
PEDOT	poly(ethylenedioxythiophene)
PTSA	p-Toluenesulfonic acid
SCE	Saturated Calomel Electrode
THF	Tetrahydrofuran
TMS	Trimethylsilane
VB	Valence Band

CHAPTER 1

INTRODUCTION

1.1 Conducting Polymers

Until the discover of partial oxidation of polyacetylene by Shirakawa, Mc Diarmid, and Heeger in 1977, polymers are known as insulators. They won the Nobel Prize for Chemistry in 2000 for the discovery and development of conducting polymers [1].

After this ground-breaking invention, the synthesis of new organic polymers that can conduct electricity has drawn considerable attention both in academia and industry. A new class of material called "synthetic metals" were achieved as a consequence of this outstanding discovery. That conjugated polymers can be transformed into compounds that can have metal like conductivity with doping process.

Despite polyacetylene demonstrated very high conductivity in the doped form, the material was unprocessable since it was unstable to oxygen and humidity. In addition to this, characterization and processing of the polymer could not be achieved due its insolubility. Thus synthetic work concentrated on increasing the processability of PAc [2]. Additionally, chemists were concentrated in the synthesis of new conducting polymers with improved properties starting in the early 1980s (Figure 1.1).

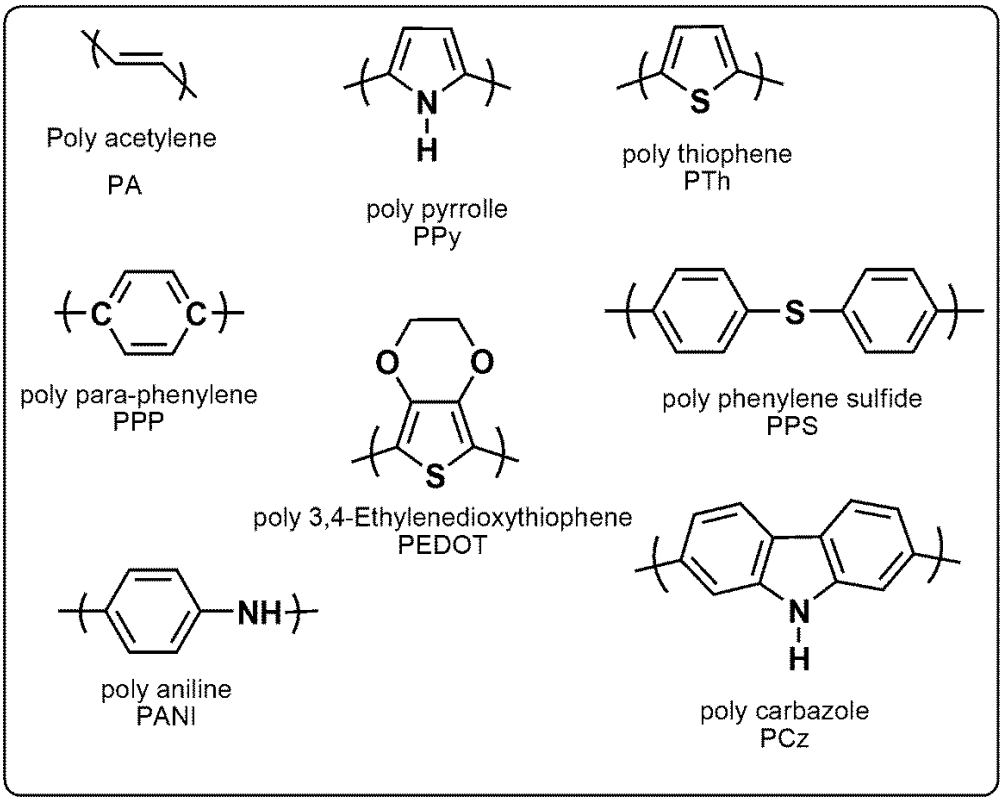

Figure 1.1. Common conducting polymer structures

In that period of time, polypyrolle [PPy] which is highly conducting [100 S/cm] , flexible, and stable was discovered. A homogenous, free-standing film of PPy was synhesized by electropolymerization [3]. Futhermore, polythiophene [4], polyaniline [5], poly [p-phenylene] [6] and poly[p-phenylene vinylene] [7] and their derivatives such as poly[3,4- ethylenedioxythiophene] [PEDOT] were examined extensively for their potential desirable properties like low oxidation potential and ease of processability compared to PAc appropriating for more diversity of structures.

Conductivities and stabilities of some of these polymers were given in Table 1.1. Even if highest conductivity was observed for polyacetylene, the stability and processability of heterocycles make them more functional.

Table 1.1 Conductivities and stabilities of some of these polymers

Polymer	Conductivity [$\Omega^{-1}cm^{-1}$]	Stability [Doped State]	Processing Possibilities
Polyacetylene	10^3-10^5	Poor	Limited
PPS	10^2	Poor	Excellent
Polypyrroles	10^2	Good	Good
Polyaniline	10^2	Good	Good
Polythiophenes	10^2	Good	Excellent
Polyphenylene	10^3	Poor	Limited
PPV	10^3	Poor	Limited

In the recent time, conjugated polymers have attracted great attention since they are promising materials for electronic applications. These materials were utilized in organic-based transistors [8], photovoltaic devices [9], organic light emitting diodes [OLEDs] [10], sensors [11-12], and electrocromic devices [13-14].

Assorted approaches have been used to design and synthesize new primer structures comprising good electrical, optical and mechanical features with processability and environmentally stable. In order to promote a specific desired feature for a specific application, a basic understanding of how structural modification is related to the material properties was needed.

Recent studies indicated that the magnitude of the band gap and position of the edges of the conduction band and valence band are most important factors to the control of conducting polymer properties. Developing methodologies to attain such precise control over the electronic band structure of the polymer is a key aspect for the advancement of the conducting polymer field.

1.2 Band Theory and Electrical Conduction Mechanism in Conjugated Polymers

1.2.1 Band Theory

Materials are classified into three categories depending on their conductivities: conductors, semiconductors and insulators. Band theory can explain the electrical behavior of conducting polymeric materials.

According to band theory, conjugated polymers constitute two discrete energy bands called as valence band (VB) which is the lowest energy containing highest occupied molecular orbital (HOMO), and conduction band (CB) defined as highest energy containing lowest unoccupied molecular orbital (LUMO).

The main difference between conductivity of materials is the bandgap (Eg) which defined as the energy spacing between valance band (VB) and conduction band (CB) [15].

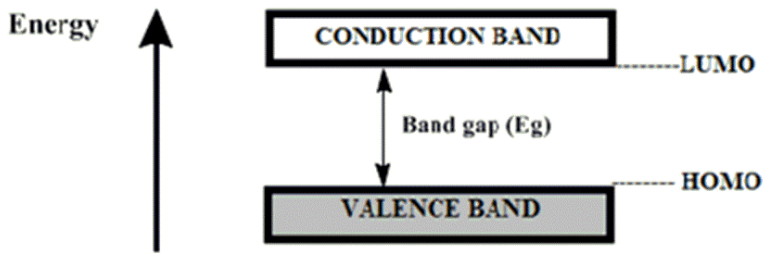

Figure 1.2. Band structure in an electronically conducting polymer

Depending on their conductivity, conjugated polymers are generally classified as semiconductors. In semiconductors there exist a small energy difference between

valence and conduction band, hence electrons can be reinforced from VB to CB via vibrational and thermal excitation or excitation by photons. In metals CB and VB have zero band gap since they are overlapped. On the other hand, for insulators that they have is a large energy difference between HOMO and LUMO levels. Owing to this case electrons cannot be promoted from VB to CB. Conjugated polymers called as semiconductors which lie between metals and insulators [16].

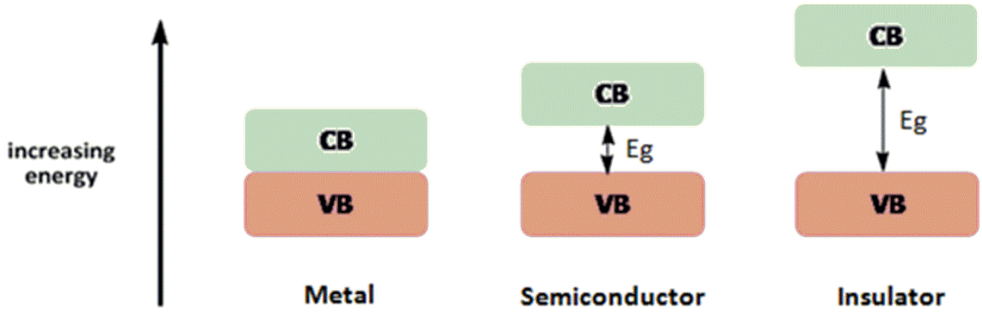

Figure 1.3. Schematic representation of metals, semiconductors and insulators

Due to the generation of interbands between valence and conduction band conducting polymers can become conductors. However, this case is possible upon doping. With doping process, π-orbitals of repeating units overlap and form continuum band levels, which leads to increased conjugation.

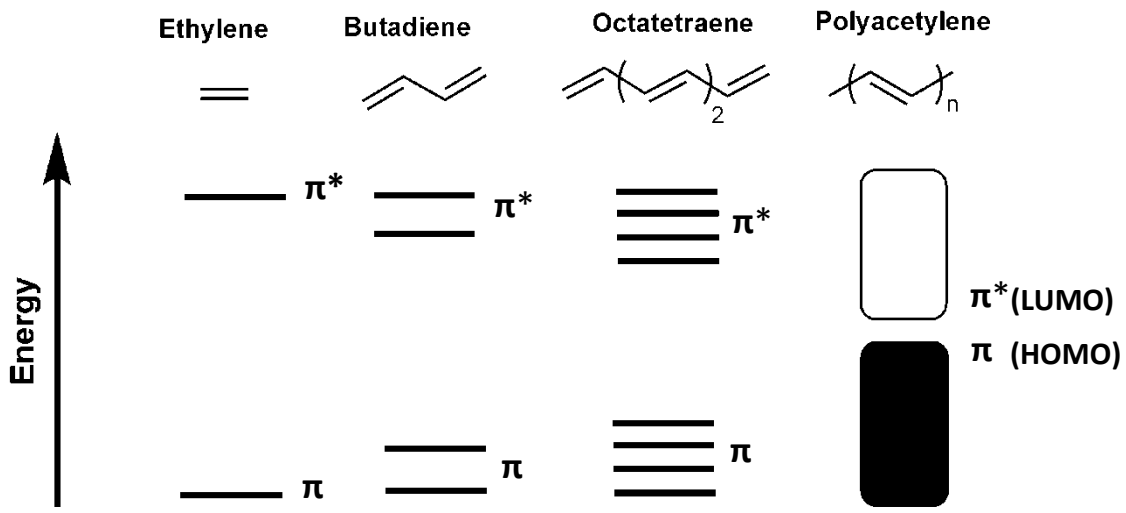

Figure 1.4. Generation of bands in conjugated polymers

1.2.2 Conduction Mechanism in Conjugated Polymers

1.2.2.1 Concept of Charge Carriers

In an attempt to understand conduction mechanism in conjugated polymers, beside band theory, the concept of soliton, polaron and bipolaron should be known. Defects on the polymer backbone such as radicals, cations and anions are result of oxidation and reduction process. Movement of these defects, called charge carriers, constitute the main notion of the conduction mechanism.

Positive (p-type) charge carriers are generated by oxidation of a conjugated polymer while reduction of the polymer cause negative (n-type) charge carriers. When an electron remove from the the top of the valence band of a conjugated polymer a radical cation is generated. On the contrary, addition of an electron to the conduction band leads to formation of a radical anion. Both of the resulting species are named as

polarons. A polaron has a spin of ½. Further removal or addition of electrons causes generation of bipolaronic states as shown in Figure 1.5.

New energy bands near the valence band are formed (bipolaronic states) and begin to overlap with increasing number of bi polarons in the polymer main chain. Thus, the band gap of the polymer become smaller and conductivity increases. Another charge defect is soliton. There are three types of solitons; neutral solitons ,positive solitons and negative solitons. Charged solitons possess no spin; whereas neutral solitons possess spin but no charge. Oxidation generates positively charged solitons by inserting an electron to the acceptor band or removing an electron from localized state of neutral soliton.

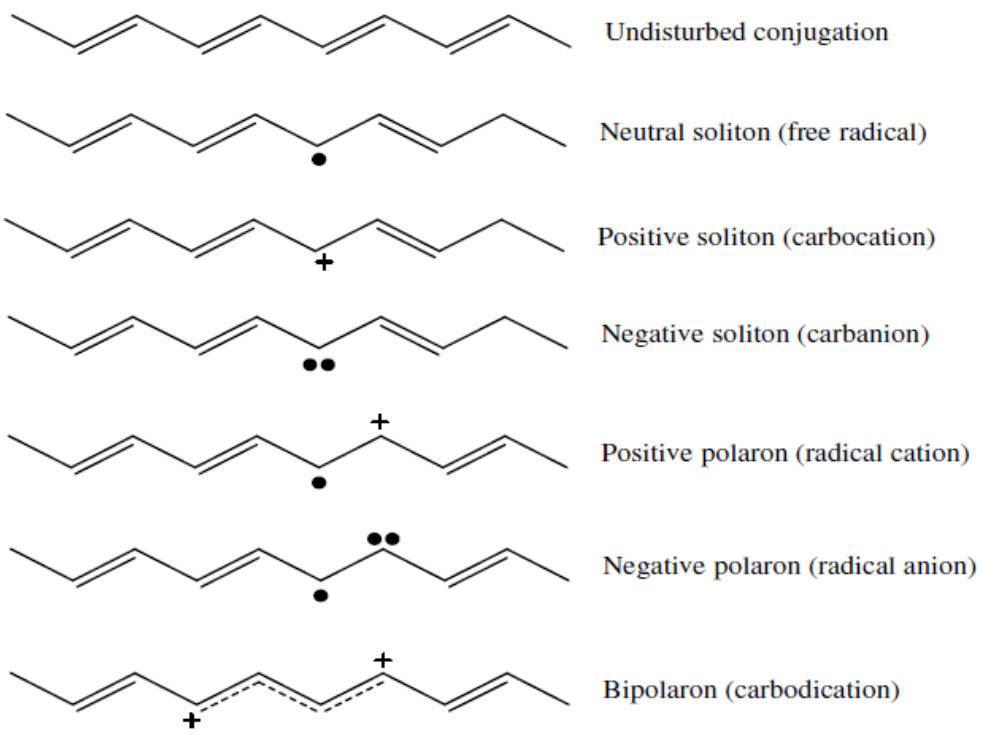

Figure 1.5. Structralal representation of soliton polaron and bipolaron of Polyacetylene

1.2.2.2 Doping Process

Doping process is the unique property that seperates conducting polymers from all other types of polymers [17]. Converting from the layout of the gap insulator or semiconductor to metal leads to enhance conjugation of conducting polymers. The process that reconstructs the neutral polymer main chain to a charged π-conjugated system is referred as "doping". Redox processes, which contain partial electron addition to or removal electron from the π-conjugated system of the polymer main chain, achieve doping of conjugated polymers [18-19]. The chemical composition of the actual polymer backbone does not change since these doping and dedoping processes are usually reversible.

Fundamentally, oxidation which is removing an electron from valence band of a neutral polymer, is described as p- doping and reduction which is adding an electron to conduction band of polymer is described as n-doping. n-Doping process is less studied than p-doping due to the requirement for rigorously dry and oxygen-free conditions [20].

Doping of a conducting polymer leads to achieve electrical charge carriers.If the doping levels regulated correctly, conductivity between nondoped (insulating or semiconductor) and fully doped (conducting) form of the polymer can easily be procured. In the doped state the main chain of a conducting polymer comprises of a delocalized π-system. On the contrary, in the nondoped state polymer backbone possesses no conjugation [21]. With p-doping process positive charges occurs on the polymer chain. When positioned in an electric field, these charges can move through the polymer chain, acting as charge carriers.

$$[P]_x + xyA^- \rightarrow [P^{y+}[A]_y]_x + xye^-$$

n-Doping in contrast, donates electrons to the polymer system as a result of reduction, producing negative charges on the polymer chain. These electrons function as current carriers and move in the polymer when positioned in an electric field.

$$[P]_x + xye^- + xyM^+ \rightarrow [P^{y-}[M^+]_y]_x$$

Chemical doping is generated on the polymer by either an electron acceptor, through oxidation [oxidant, A] or an electron donor, through reduction [reductant, B];

$$\text{p-doping} \qquad [P]_n + A \rightarrow [P]_n{+}A^-$$

$$\text{n-doping} \qquad [P]_n + B \rightarrow [P]_n^- B^+$$

where A^- and B^+ are the doping ions. Chemical oxidation/reduction can occur by the exposure of the polymer to I_2 or AsF_5 vapors, $FeCl_3$ or $CuCl_2$. The doping level can be regulated by the vapor pressure of the dopant or its concentration, the temperature of the reaction, the doping time, and the type of the polymer.

Electrochemical doping is a more desirable process than chemical doping due to the several advantages such as better control over the doping level. Any doping level can be achieved by applying a constant potential over a length of time, and the level at which the polymer is doped is directly related to the voltage.

1.2.2.3 Hopping

Basically, mobility of the charge carriers determines the conductivity of conjugated polymers. By virtue of doping process, there exist a great many of carriers on the polymer backbone, however their mobility determines the level of conductivity of the polymer [22]. Mobility of electrical charges on conducting polymer occurs in three ways. Charges can move along the polymer backbone (intrachain movement), jump to neighbor polymers or variable range hopping can take place (interchain movement). Effective conjugation of the polymer regulates the level of intrachain movement, while interchain movements are connected to the stacking of the polymers. Temperature affects mechanism of variable range hopping in a manner which allows their characterization. Mott model states the conductivity as;

$$\sigma = \sigma_0 \exp [-(T_o/T)]^{\gamma}$$

with T_0 is given by $T_0 = 1 / (k\varepsilon N (E_F)$ where k is the Bolztmann's constant and N (E_F) is the density of the states at the Fermi level, σ_0 is the conductivity at absolute zero (0 ^{0}K), T is the temperature and $^{\gamma}$ is a factor of the dimensionality [d] of the hopping process

$$^{\gamma} = 1/ (1 + d)$$

Dimensionality of the hopping process of most polymers is 3-D, hence a linear log σ vs. $T^{-1/4}$ is an evidence of variable range hopping process.

1.3 Synthesis Of Conducting Polymers

Several numbers of approaches such as chemical, electrochemical, photochemical, concentrated emulsion, inclusion, solid-state and plasma pyrolysis polymerizations are used to synthesize conducting polymers. However, chemical and electrochemical polymerizations are extensively employed techniques. Conducting polymers which are stable in both doped and undoped states and soluble in common solvents were synthesized to achieve new and novel structures, where the order of the polymer backbone as well as conductivity was increased.

1.3.1 Chemical Polymerization

Chemical polymerization is the most widely used technique to synthesize conducting polymers. This technique is also the least and most simple. [23-24]. $FeCl_3$ is generally used as the chemical oxidant to polymerize heterocyclic monomers such as aniline, thiophene, pyrrole etc. Strong bases such as ammonium hydroxide or hydrazine is used to reduce the polymer to its neutral state. Chemical polymerization takes place in th bulk of the solution, and the resulting polymers generally precipitate since they are generally insoluble [25]. In Figure 1.6 oxidative polymerization of a heterocyclic compound with $FeCl_3$ is shown [26].

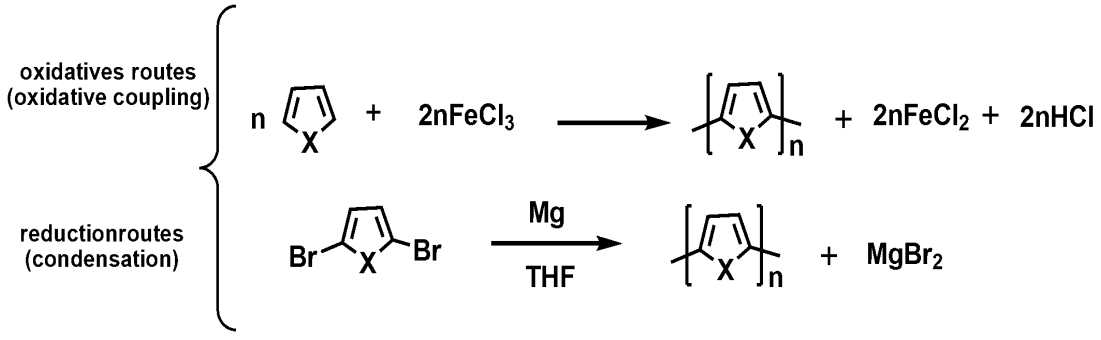

Figure 1.6. Oxidative polymerization of a heterocyclic compound with $FeCl_3$

1.3.2 Electrochemical Polymerization

Electrochemical polymerization which has several advantages. One major advantage is the ability to produce the polymer on an electrode in a simple selective and reproducible way. By the virtue of deposition charge, the method permits easy control of the film thickness. In this type of polymerization, doping of the polymer and processing occur in sequence in one pot. Firstly, the polymer synthesis is achieved and secondly doping and processing are followed. It can be concluded that electrochemical polymerization is the most important technique for fundamental studies regarding synthesis and properties of the corresponding polymers [27].

1.3.2.1 Mechanism of Electropolymerization

By applying positive potential [oxidation] to various resonance stabilized aromatic molecules such as thiophene, furan, selenophene, pyrrole etc., conductive polymers can be achieved. It has been suggested that the polymerization contain either radical-cation/radical cation coupling or reaction of a radical cation with a neutral monomer (Figure 1.7) [28-29].

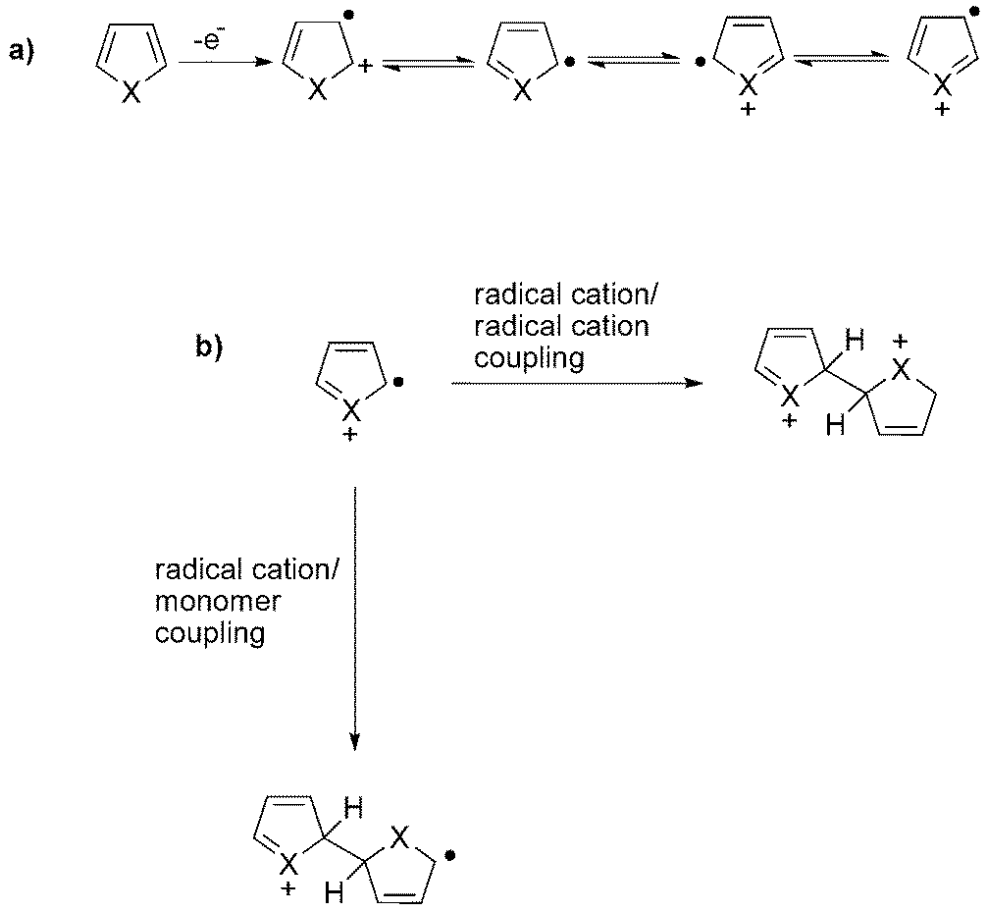

Figure 1.7. a) Resonance stabilization of a five membered heterocyclic compound upon formation of radical-cation **b)** Radical-cation/monomer and radical cation/ radical cation coupling where X = N-H, S, O

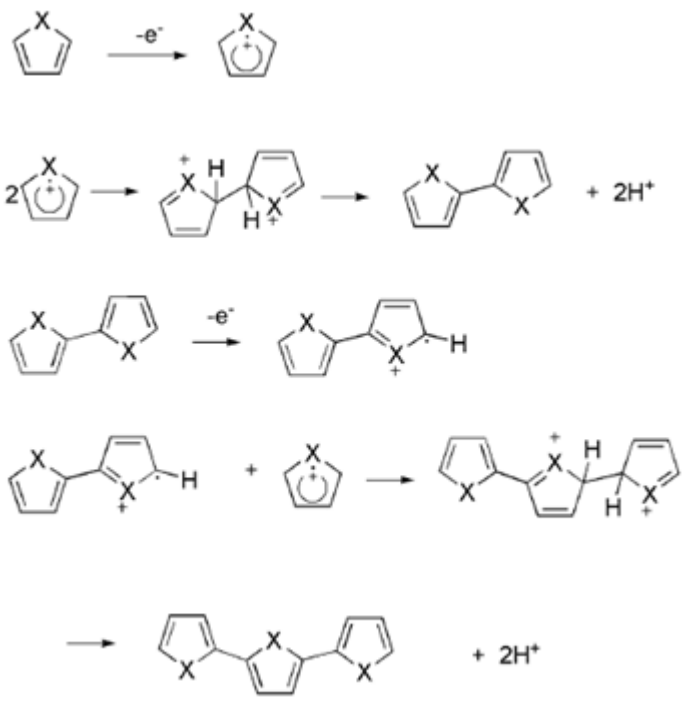

Figure1. 8. Electropolymerization mechanisms of heterocycles [X = S, O, NH]

Figure 1.8 demonstrates the mechanism recommended for the electropolymerization of heterocycles by anodic coupling. Firstly, electropolymerization (E) initiates polymerization with the oxidation of the monomer and generates its radical cation. The electron-transfer reaction is much faster than the diffusion of the monomer from the bulk solution which provides that the solution in the vicinity of the electrode surface has a high concentration of radicals continuously. Secondly, coupling pursues the first step. Coupling may progress by way of two different directions which are the addition of radical cation to heterocyclic monomer or the combination of two radical cations due to its properties second step is contentious step. In the act of radical-radical coupling, dihydro dimer dication is generated which then loses two protons and rearomatizes. This rearomatization creates the propellant of the chemical step (C). Owing to the applied potential, the dimer exists in its radical form

and undergoes further coupling with a monomeric radical. In a radical-monomer coupling mechanism, the radical cation and monomer react with each other to produce neutral dimer by the loss of another electron and two protons. The dimer and subordinated oligomers are more easily oxidized than the monomer and the resulting dimer radical cation occurs further coupling reactions, proton loss and re-aromatization. Electropolymerization advances through successive electrochemical and chemical steps according to a general ECE (E for electrochemical, C for chemical), until the oligomers become insoluble in the electrolyte solution and precipitate onto the electrode surface.

1.3.2.2 Effects of Electrolytic Media on Electrochemical Polymerization

There exist several important effects of electrolytic media on electrochemical polymerization such as temperature, solvent, electolyte and total amount of applied current. Electrical properties and the morphology of the polymer can be greatly affected by these parameters.

A solvent with a high dielectric constant, to dissolve supporting electrolyte is a favorable media for polymerization. The solvent should also be stable at the applied potential and should not have nucleophilic character since reactive radicals are produced during oxidative electrochemical polymerization.

Electrolytes should be non-nucleophilic and electrochemically inactive. They also play an important part in the doping process of the polymers where the anion of the electrolyte serves as the counter anion of the positive charge that is generated on the polymer backbone. In order to synthesize conducting polymers, tetraalkylammonium or lithium salts of perchlorates, hexafluorophosphates and tetrafluoroborates are commonly preferred [30].

Side reactions of radical cations or oxidized polymer with nucleophiles can occur. In order to reduce these cases the concentration of monomers is kept high [0.1M].

Millimolar concentrations of monomers can be used with decreasing number of side reactions.

This could be possible if oxidation potential of monomer is low enough [31]. Electrochemical polymerizations are performed with inert electrodes such as gold, platinum, indium-thin-oxide (ITO) coated glass. Ag/Ag^{+}, Ag wire and saturated calomel electrode (SCE) can be used as reference electrodes.

1.4 Characterization of Conducting Polymers

In order to characterize conducting polymers, a diversity of analytical techniques can be exercised. Cyclic voltammetry is an effective technique for understanding redox process in conducting polymers. Structure confirmation, molecular motion and chain orientation of soluble polymers are investigated by nuclear magnetic resonance. Molecular weight is specified via gel permeation chromatography (GPC). In order to determine glass-transition and melting and decomposition temperatures differential scanning calorimetry and thermogravimetric analyses are used. Fourier transform infrared spectrometry (FTIR) is used to understand functional groups and doped ions in the polymer chain. X-ray photoelectron spectroscopy (XPS) can be used for structure analysis.

1.5 Application Areas of Conducting Polymer

Conducting polymers, which demonstrate novel features, have number of applications in many areas. Owing to their excellent properties such as flexibility, low cost, high electrical conductivity and boundless diversity of the structures drew a great attention from researchers. These properties also clarify the great efforts on conducting polymer application researches. Conjugated polymers are employed as semiconductors in electronic devices such as solar cells, field effect transistors [32] and light emitting diodes [33]. Electronic conductors, electromagnetic shielding materials and electrostatic dissipation materials made from conjugated polymers in doped state. Moreover, the reversible switching between neutral and doped states of conjugated polymers make possible construction of electrochromic devices, battery

electrodes and biosensors. Color, conductivity and volume of conjugated polymers change with switching between doped and dedoped states. Applications that utilize these properties include battery electrodes, mechanical actuators, sensors, drug delivery and electrochromics [34-35].

1.6 Chromism

Color change of materials associated with external stimulus is describes as chromism. Chromic behavior is one of the characteristics of conducting polymers. There exist a number of types of chromism reported in the literature for CPs such as solvatochromism, ionochromism, thermochromism, piezochromism. The reason of these different chromic behaviors is the energy change in π-π^* transition band gap and conformational modification induced by the consecutive environmental changes such as solvent power, ion strength, temperature and pressure, respectively [36].

1.6.1 Electrochromism

Electrochromisim is mainly described as the reversible optical change of a material monitored upon alternation of the applied potential. An electrochromic material can be defined as a material that changes color in a steady but reversible manner by an electrochemical oxidation-reduction reaction. Color changes generally occur between the two colored states or a colored and a transparent state. In some cases when more than two redox states are electrochemically available, the electrochromic material may demonstrate several colors and these types of polymers are named as multichromic [37]. Essentially, there are three categories of electrochromic materials are known; metal oxides, molecular dyes and conducting polymers. Tungsten trioxide (WO_3) is the most widely used metal oxide.

The doping process leads to a change in the structure of conducting polymers. Energies of electronic transitions are decreased in comparison with aromatic neutral forms. If the electronic transitions take place in the visible region, color changes are observed. Due to the motions of anions and cations in the polymer backbone doping and dedoping processes form synchronously with a mass transport. Color change kinetics is determined with the slower process [38].

1.6.2 Types of Electrochromic Materials

There exist three essential types of electrochromic materials in recognition of their electronically accessible optical states.

The first class of materials with at a minimum one colored and one bleached state. Optical shutters and smart windows are absorption/transmission type device applications. The first class of electrochromic materials are especially useful for these kind of applications. Representative examples in this field are viologens, metal oxides and polymers such as poly(3,4-ethylenedioxythiophene) (PEDOT).

The second type includes materials with two distinctive colored states. These materials are used in display-type applications where different colors are desired in different redox states. For instance polythiophene can be a good candidate for this type applications owing to its colored states which switch from red to blue.

The third class of materials consist of polymers the that can achieve more than two color states depending on the redox state of the material. There is a growing interest in the electrochromic area for these type of materials due to their versatility for making blends, laminates, and copolymers [39].

Window application is a device that cycled between transparent and colored states is one of the more favorable and outstanding uses for electrochromic polymers. Also, as the range of convenient colors in electrochromic polymers proceeds, these materials should become more useful for display technology [40].

Electrochromic materials have gained great attention for their potential use in the infrared and microwave regions besides smart windows, storage devices, and displays [41].

1.7 Spectroelectrochemistry

Electronic and optical changes of conducting polymers are monitored via spectroelectrochemistry technique during electrochemical processes. It provides information about electronic band gap and intraband states formed upon doping.

Conducting polymers called as an insulators that have a band gap, Eg, between the valence band (HOMO) and the conduction band (LUMO) in their neutral state. Upon doping (or oxidizing), lower energy intraband transitions formed and polarons and bipolarons are occured simultaneously. Due to this processes the conductivity is increased. In order to investigate formation of π to π^*, polaronic and bipolaronic transitions and calculation of band gap energy, spectroelectrochemistry is essentially important.

1.8 Electrochromic contrast and Switching Speed

Electrochromic materials have several important characteristics. However, electrochromic contrast and switching speed are among the most important characteristics of electrochromic materials.

Electrochromic contrast is defined as the percent transmittance change (%ΔT) between the oxidized and reduced states. Percent transmittance is calculated at a specified wavelength where the polymers have the highest optical contrast [42].

Switching time is described as the time required for the investigation of optical changes for the redox states of conducting polymers. There are several factors such as accessibility of the ions to the electroactive sites, magnitude of the applied

potential, ionic conductivity of the electrolyte, film thickness, and morphology of the film affectes the switching speed [42].

1.9 Donor-Acceptor Theory and Low Band Gap Systems

π- Conjugated polymers with donor-acceptor moieties have attracted a great attention in recent years, because, manipulation of the HOMO-LUMO levels of the polymer can make it possible to built small band-gapped semiconducting polymers. Since the neutral conductivity of CPs could be increased via a decrease in the band gap, synthesis of materials with small band gap is very important. In order to realize bipolar charge transport materials for light-emitting diodes, lasers and other applications and systems with efficient photoinduced charge transfer and separation for photovoltaic devices donor-acceptor type conjugated polymers' uses have been enhanced. Additionally, band gap also affect the color of the polymer. In doped state transparent polymers are important materials and this rare property can also be satisfied by modification of band gap.

Most of conducting polymers reported in the literature up to present have band gap values higher than 2 eV and they are named as mid-to high band gap polymers. If band gaps of the polymers are lower than 1.5 eV they are classified as low band gap materials. However, there are few examples in the literature about polymers with band gap below 0.8 eV [43].

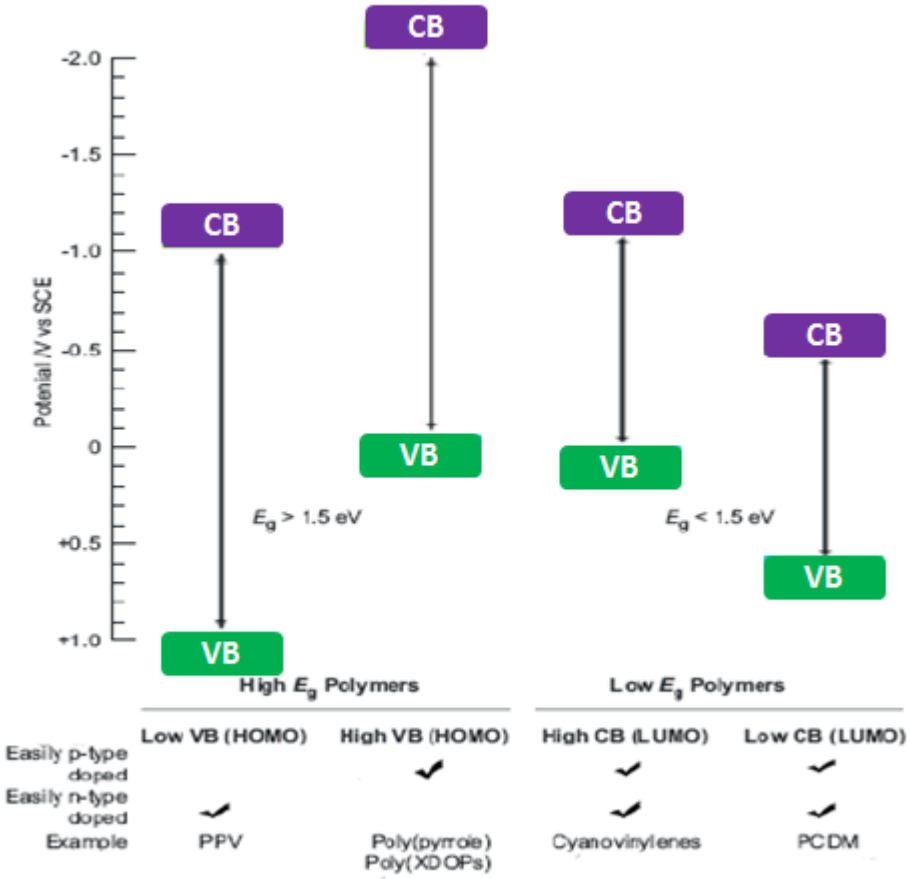

Figure 1.9. Possibilities for positioning of bond edges in both high and low band gap polymers

Band gap is also used to identify the easiness of doping process and the stability in doped states compared to neutral forms of polymer.

There have been several methodologies for modification of the band gaps. The five main approaches are;

Controlling bond-length alternation (Peierls Distortion),

Creating highly planar systems,
Inducing order by interchain effects,
Resonance effects along the polymer backbone,
Donor-Acceptor Approach

When compared to all of them with each other donor-acceptor approach comes into prominence among them since this method minimize solubility problems and also provides variety in synthesis [44].

Donor-acceptor theory is the coupling of electron rich donor and electron deficient acceptor units. For the synthesis this kind of polymers, the donor and acceptor moieties and their appropriate match have great importance. A study by Thomas et al. represent this effect using cyanovinylene as the acceptor unit with five different donor units. The results of this study are demonstrated in Figure 1.9. When cyanovinylene is the acceptor unit, if we increase the electron donor ability of donor group, D-A match will be better and this proper match will lower band gap to 1.1 eV [45].

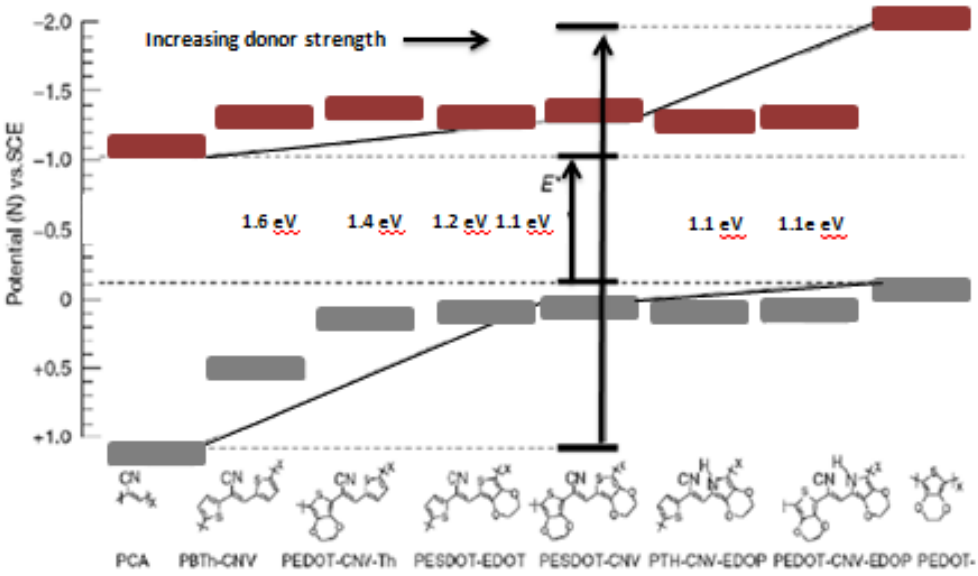

Figure 1.10. VB and CB levels for cyanovinylene substituted with different donor groups

CHAPTER 2

EXPERIMENTAL

2.1 Materials And Methods

All chemicals and solvents to synthesize monomers, M1 and M2, were purchased from commercial sources. Tetrahydrofuran [THF] was dried over benzophenone and sodium. Benzothiadiazole [Sigma-Aldrich], bromine [Br_2] [Sigma-Aldrich], hydrobromic acid [HBr, 47 %] [Merck], sodium borohydride [$NaBH_4$] [Sigma-Aldrich], thienothiophene [Sigma-Aldrich], bis[triphenylphosphine]palladium[II] dichloride [$Pd[PPh_3]_2Cl_2$] [Sigma-Aldrich], n-Butyllithium [n-BuLi] [Acros] , tributyl tinchloride [$SnBu_3Cl$] [Sigma-Aldrich], ethanol [EtOH] [Sigma-Aldrich], dichloromethane [DCM] [Sigma-Aldrich], hexane [Sigma-Aldrich] were used as received.

4,7-Dibromo-2,1,3-benzothiadiazole, 3,6-dibromobenzene-1,2-diamine, 1,2-bis[decyloxy]benzene, 1,2-bis[3,4-bis[decyloxy]-phenyl]ethane-1,2-dione tributyl[thieno[3,2-b]thiophen-2-yl]stannane, 4,7-dibromobenzo[c][1,2,5]selenadiazole, 2,3-bis[3,4-bis[decyloxy]phenyl]-5,8-dibromoquinoxaline, were synthesized with previously described procedures.

2.2 Equipment

Structures of monomers and polymers were analyzed with NMR. ^{1}H and ^{13}C NMR were recorded on Bruker Spectrospin Avance DPX-400 Spectrometer with TMS as internal standard. For electrochemical studies , Gamry potentiostat in a three electrode system were used. Indium Tin Oxide (ITO) coated glass was used as the working electrode, Ag wire was used as the pseudo reference electrode (Fc/Fc+(0.3V)) and Pt wire used as counter electrode. The electrolytes were 0.1 M $NaClO_4$-$LiClO_4$ in acetonitrile (ACN) . Highest occupied molecular orbital (HOMO) and lowest unoccupied molecular orbital (LUMO) energy levels were calculated by taking normal hydrogen electrode (NHE) values as -4.75 eV. Spectroelectrochemical studies were performed by Varian Cary 5000 UV-Vis spectrophotometer.

2.3 Procedure

2.3.1 Synthesis

2.3.1.1 Synthesis of 4,7-dibromo-2,1,3-benzothiadiazole (1)

Bromination of benzothiadiazole was synthesized according to the previously reported procedure in the literature. [47] Benzothiadiazole (5.00 g, 36.7 mmol) was dissolved in HBr (47%, 90 mL). HBr (47%, 40 mL) and Br_2 (4 mL) were mixed and added to the reaction mixture dropwise. After addition was completed the mixture was refluxed for 6 h. The mixture of reaction was cooled with an ice bath and waited for forming precipitate approximate 2 h. Precipitate was filtered and washed with saturted solution of $NaHSO_3$ to clear away excess Br_2. Precipitate was dissolved in dichloromethane and extract with water. Organic part of extraction was dried over $MgSO_4$ and solvent was removed under reduced pressure. Yellow solid was obtained with a yield of 95%. (10.22 g, 34.78 mmol).

^{1}H NMR (400 MHz, $CDCl_3$): δ (ppm) 7.66 (s, 2H)

^{13}C NMR (100 MHz, $CDCl_3$): δ (ppm) 152.76, 132.15, 113.70

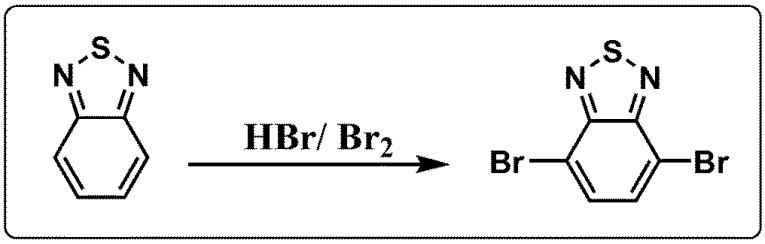

Figure 2.1. Synthetic route for 4,7-dibromo-2,1,3-benzothiadiazole

2.3.1.2 Synthesis of 3,6-dibromobenzene-1,2-diamine (2)

Reduction of brominated benzothiadiazole was achieved according to the previously reported procedure in the literature [48]. 4,7-Dibromo-2,1,3-benzothiadiazole **(1)** (4.00 g, 13.60 mmol) was dissolved in ethanol. $NaBH_4$ (20.0 g, 528 mmol) was slowly added to the mixture. When the addition was completed the reaction mixture was stirred overnight at room temperature. Ethanol was removed under reduced pressure. The crude product was dissolved in diethyl ether and washed with brine and water respectively. The organic layer was dried over $MgSO_4$ and the solvent was removed under reduced pressure to give **2** (3.47 g, 90%.).

^{1}H NMR (400MHz, $CDCl_3$): δ (ppm) 3.82 (s, 4H), 6.78 (s, 2H)

^{13}C NMR (100MHz, $CDCl_3$): δ (ppm) 131.69, 121.22, 107.65

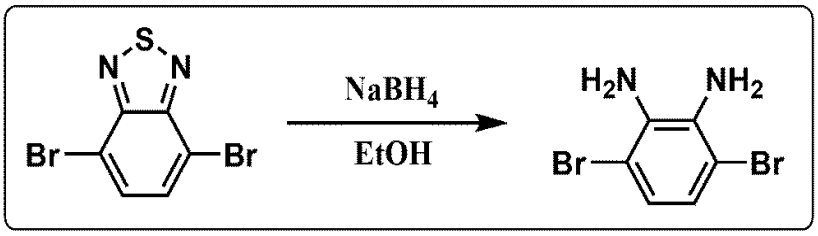

Figure 2.2. Synthetic route for 3,6-dibromobenzene-1,2-diamine

2.3.1.3 Synthesis of 1,2-bis[decyloxy]benzene (3)

1,2-Bis[decyloxy]benzene was synthesized according to the previously reported procedure in the literature [49]. Catechol (5.00 g, 45.0 mmol) and K_2CO_3 (19.0 g, 137 mmol) was dissolved in 30 mL DMF and brought to reflux, 1-bromodecane (26.65 g, 120.0 mmol) was then added to the reaction mixture. The reaction was stirred under argon atmosphere for 40 h. When the reaction complete (TLC), DMF was removed under reduced pressure. Water was added to the residue and the mixture was extracted with DCM. Organic layer was dried ($MgSO_4$) and the solvent was evaporated.. The product was precipitated with cold methanol and then filtrated.

^{1}H NMR (400 MHz, $CDCl_3$): δ (ppm) 6.88 (s, 4H), 3.99 (t, J=6.7 Hz, 4H), 1.81 (m, J=6.8 Hz, 4H), 1.46 (m, J=6.6 Hz, 4H), 1.27 (m, J=8.1 Hz, 24H), 0.88 (t, J=7.0 Hz, 6H)

^{13}C NMR (100 MHz, $CDCl_3$): δ (ppm) 149.3, 121.0, 69.33, 31.92, 29.64, 29.59, 29.45, 29.40, 26.06, 22.69, 14.11

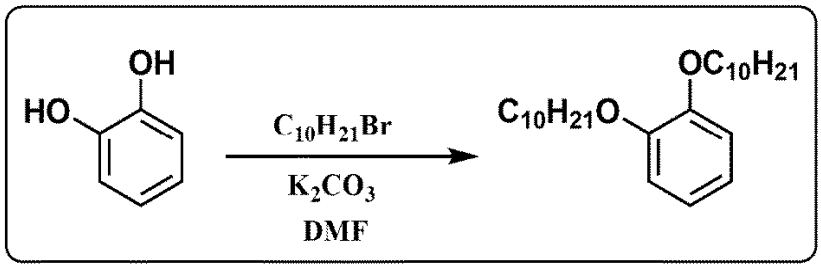

Figure 2.3. Synthetic route for 1,2-bis[decyloxy]benzene

2.3.1.4 Synthesis of 1,2-bis[3,4-bis[decyloxy]-phenyl]ethane-1,2-dione (4)

1,2-Bis[3,4-bis[decyloxy]-phenyl]ethane-1,2-dione was synthesized according to the previously reported procedure in the literature [49]. Firstly, 1,2-bis[decyloxy]benzene **(3)** (1.00 g), $AlCl_3$ (377 mg) and CS_2 (6.50 mL) was mixed under argon atmosphere. After 15 min. the mixture was cooled to 0 $^{\circ}$C and a mixture of oxalyl chloride (0.13 mL) and CS_2 (1.3 mL) was added to the reaction slowly. The reaction was stirred overnight at room temperature. When the reaction complete (TLC), the mixture washed with ice-water and filtrated.

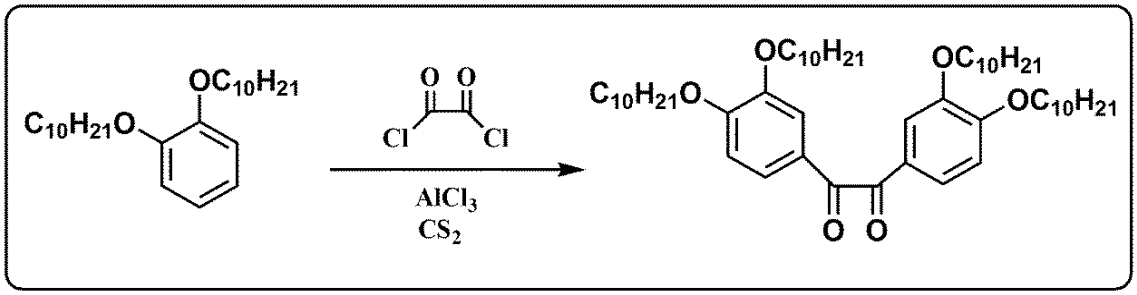

Figure 2.4. Synthetic route for 1,2-bis[3,4-bis[decyloxy]-phenyl]ethane-1,2-dione

2.3.1.5 Synthesis of tributyl[thieno[3,2-b]thiophen-2-yl]stannane (5)

Stannylation of thieno[3,2-b]thiophene was performed according to the previously reported procedure in the literature [50]. Thieno[3,2-b]thiophene (5.0 g) was dissolved in THF. After cooling the solution to -78^{o}C, n-BuLi (22.3 mL, 35.6 mmol) was added to the solution very slowly. Then tributyltin chloride (11.66 g, 35.66 mmol) was added drop wise at -78 ^{o}C. The mixture was stirred overnight at room tempreture. THF vas removed under reduced pressure. Water was added and the mixture was extracted with DCM. Combined organic layers were dried ($MgSO_4$) and the solvent was evaporated to give **5**.

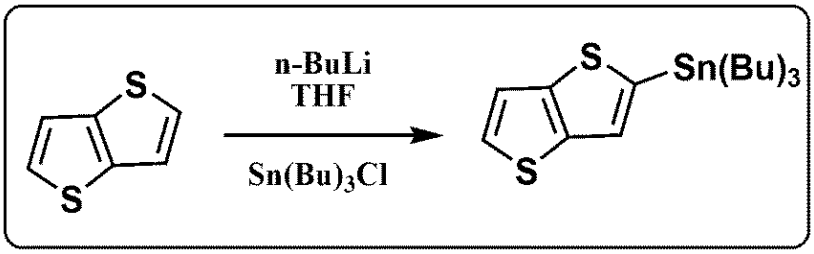

Figure 2.5. Synthetic route for tributyl[thieno[3,2-b]thiophen-2-yl]stannane

2.3.1.6 Synthesis of 4,7-dibromobenzo[c][1,2,5]selenadiazole (6)

4,7-Dibromobenzo[c][1,2,5]selenadiazole was synthesized according to the previously reported procedure in the literature. [51] 3,6-Dibromobenzene-1,2-diamine (**2) (** 1.00 g, 3.70 mmol) was dissolved in EtOH (20.5 mL) and heated to reflux. The mixture of SeO_2 [0.43 g, 3.80 mmol]and hot water (8.20 mL) was added to the solution. The mixture was heated under reflux for 2 h. Filtration of the yellow precipitate gave 4,7-Dibromobenzo[c][1,2,5]selenadiazole (0.9 g) in 80% yield.

^{1}H NMR (400MHz, $CDCl_3$): δ (ppm) 7.65 (s,2H)

^{13}C NMR (100MHz, $CDCl_3$): δ (ppm) 132.18

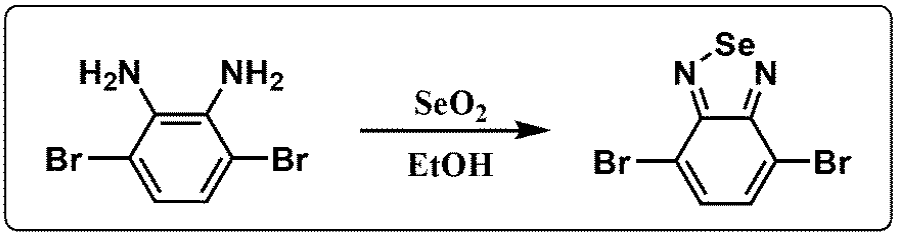

Figure 2.6. Synthetic route for 4,7-dibromobenzo[c][1,2,5]selenadiazole

2.3.1.7 Synthesis of 2,3-bis[3,4-bis[decyloxy]phenyl]-5,8-dibromoquinoxaline (7)

2,3-Bis[3,4-bis[decyloxy]phenyl]-5,8-dibromoquinoxaline was synthesized according to the previously reported procedure in the literature. [52] A solution of 1,2-bis[3,4-bis[decyloxy]phenyl]ethane-1,2-dione **(4)** (600 mg, 2.30 mmol) and 3,6-dibromo-1,2-phenylenediamine **(2)** (184 mg, 2.30 mmol) in ethanol (30 mL) was refluxed with a catalytic amount PTSA. After completing the reaction, the precipitate was filtered and washed with ethanol to give **7**.

^{1}H NMR (400MHz, $CDCl_3$): δ (ppm) 7.21 (d, J=1.97 Hz, 2H), 6.75 (d, J=8.86 Hz, 2H), 3.94 (m, J=6.66 Hz, 2H), 1.76 (t, J=7.20 Hz, 2H), 1.67 (m, J=7.30 Hz, 2H)

^{13}C NMR (100MHz, $CDCl_3$) δ:132.54, 123.41, 69.13, 31.94, 29.71, 29.64, 29.61, 29.41, 29.45, 29.37, 29.20, 29.10, 26.03, 22.70, 14.12

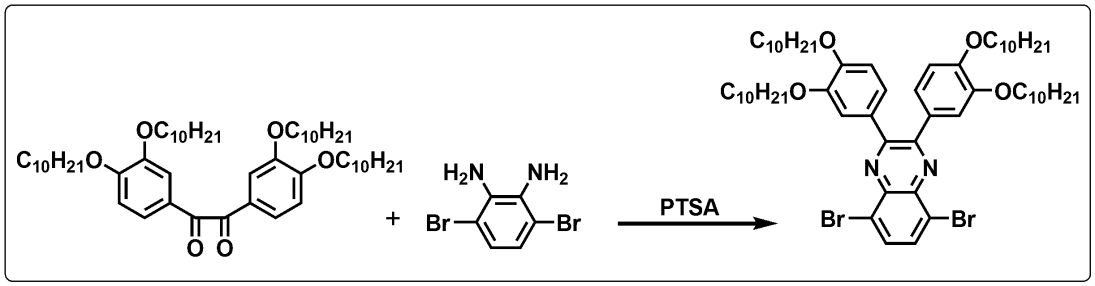

Figure 2.7. Synthetic route for 2,3-bis[3,4-bis[decyloxy]phenyl]-5,8-dibromoquinoxaline

2.3.1.8 Synthesis of 4,7-di[thieno[3,2-b]thiophen-2-yl] benzo[c][1,2,5]selenadiazole (BseTT)

4,7-dibromobenzo[c][1,2,5]selenadiazole **(6)** (200 mg, 0.60 mmol) and tributyl[thieno[3,2-b]thiophen-2-yl]stannane **(5)** (515.2 mg, 1.2 mmol) were dissolved in dry THF (100 mL). The mixture was degased with argon for 30 min. and $Pd(PPh_3)_2Cl_2$ (50 mg, 0.071 mmol) was added at room temperature under an inert atmosphere. The mixture was stirred at 100 ^oC under argon atmosphere for 15 h, cooled and concentrated on the rotary evaporator. The residue was subjected to column chromatography to afford dark purple solid (silica gel, $CHCl_3$: hexane, 1:1).

^1H NMR (400MHz, $CDCl_3$): δ (ppm) 8.33 (s,2H), 7.73 (s,2H), 7.38(d, J= 5.2 Hz, 2H), 7.23 (d, J= 5.3Hz, 2H)

^{13}C NMR (100 MHz, $CDCl_3$): δ (ppm) 162.6, 146.7, 146.1, 138.4, 134.9, 131.2, 131.1,130.9, 127.4, 127.3, 118.4

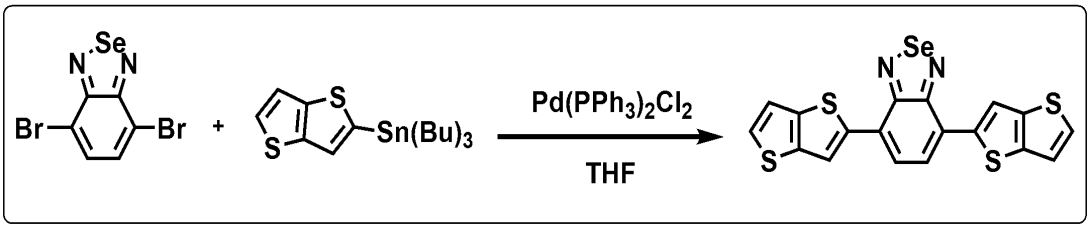

Figure 2.8. Synthetic route for 4,7-di[thieno[3,2-b]thiophen-2-yl]benzo[c][1,2,5]selenadiazole

2.3.1.9 Synthesis of 2,3-bis[3,4-bis[decyloxy]phenyl]-5,8-di[thieno[3,2-b]thiophen-2-yl]-2,3-dihydroquinoxaline (QTT)

2,3-Bis[3,4-bis[decyloxy]phenyl]-5,8-dibromoquinoxaline **(7)** (200 mg, 0.2 mmol) and tributyl[thieno[3,2-b]thiophen-2-yl]stannane **(5)** (171.7 mg, 0.4 mmol) were dissolved in dry THF (100 mL). The mixture was degased with argon for 30 min. and $Pd(PPh_3)_2Cl_2$ (50 mg, 0.071 mmol) was added at room temperature under an inert atmosphere. The mixture was stirred at 100 ^oC under argon atmosphere for 15 h, cooled and concentrated on the rotary evaporator. The residue was subjected to column chromatography to afford an orange solid (silica gel, $CHCl_3$: hexane 1:1).

^1H NMR (400MHz, $CDCl_3$): δ (ppm) 8.06 (d, J= 6.9Hz, 2H), 7.47(s, 2H),7.35 (d, J=5.2 Hz, 2H), 7.22 (d, J=5.2 Hz, 2H), 7.16(s, 2H), 6.77 (d, J=8.4 Hz, 2H), 3.97 (t, J=6.6Hz, 8H), 3.92(d, J=6.6Hz, 8H), 1.77(m, J=7.9Hz, 30H), 1.44(m, J=7.6Hz, 8H), 0.82 (t, J=4.4Hz, 30H).

^{13}C NMR (100 MHz, $CDCl_3$): δ (ppm) 163.6, 154.5, 149.2, 141.5, 132.5, 126.5, 122.5, 118.5, 117.8, 114.7, 111.8, 68.22, 68.15, 30.92, 29.88, 28.78, 28.71, 28.65, 28.60, 28.47, 28.45, 28.39, 28.35, 28.28, 25.16, 25.07, 21.68, 13.09.

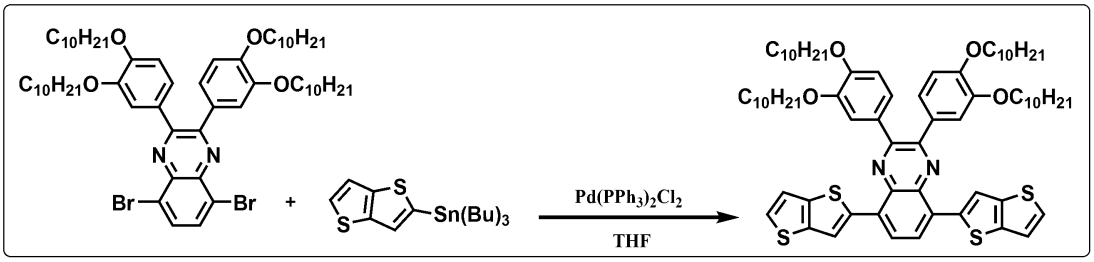

Figure 2.9. Synthetic route for 2,3-bis[3,4-bis[decyloxy]phenyl]-5,8-di[thieno[3,2-b]thiophen-2-yl]-2,3-dihydroquinoxaline

CHAPTER 3

RESULTS AND DISCUSSION

3.1 Electrochemical and Electrochromic Properties of Thienothiophene Derivative Polymers

To get a deeper perspective on the electrochemical and spectroelectrochemical properties of conjugated polymers, different methods have been conducted as a further characterization and results are summarized in this section.

Cyclic voltammetry (CV) studies were performed both for electrochemical polymerization of monomers and also to investigate the redox properties of the electrochemically synthesized polymers. The system consists of a potentiostat and a cell bearing indium tin oxide (ITO) coated glass plate as working electrode, platinum wire as counter and Ag wire pseudo reference electrodes.

3.1.1 Electrochemical and Electrochromic Properties of PBSeTT (P1)

3.1.1.1 Electrochemistry of BSeTT (M1)

BSeTT was polymerized potentiodynamically on ITO coated glass slide. Electrochemical polymerization of **BSeTT** was performed in a 0.1 M NaClO4/ $LiClO_4$ /ACN:DCM (acetonitrile: dichloromethane) (95:5) solution. . The cyclic voltammogram for electrochemical polymerization of BSeTT were reported Figure 3.1 which were scanned between 0.0 V/ 1.6 V at a scan rate of 100 mV s^{-1}.

In the first cycle of CV the irreversible monomer oxidation peak was recorded at 1.39 V for **BSeTT**. Then, after each successive cycles formation a new reversible redox couple with an increasing current intensity were observed which clarify the formation of electroactive polymer films on ITO surface. (Figure 3.1) Electrochemical polymerization of **BSeTT** was carried out successfully.

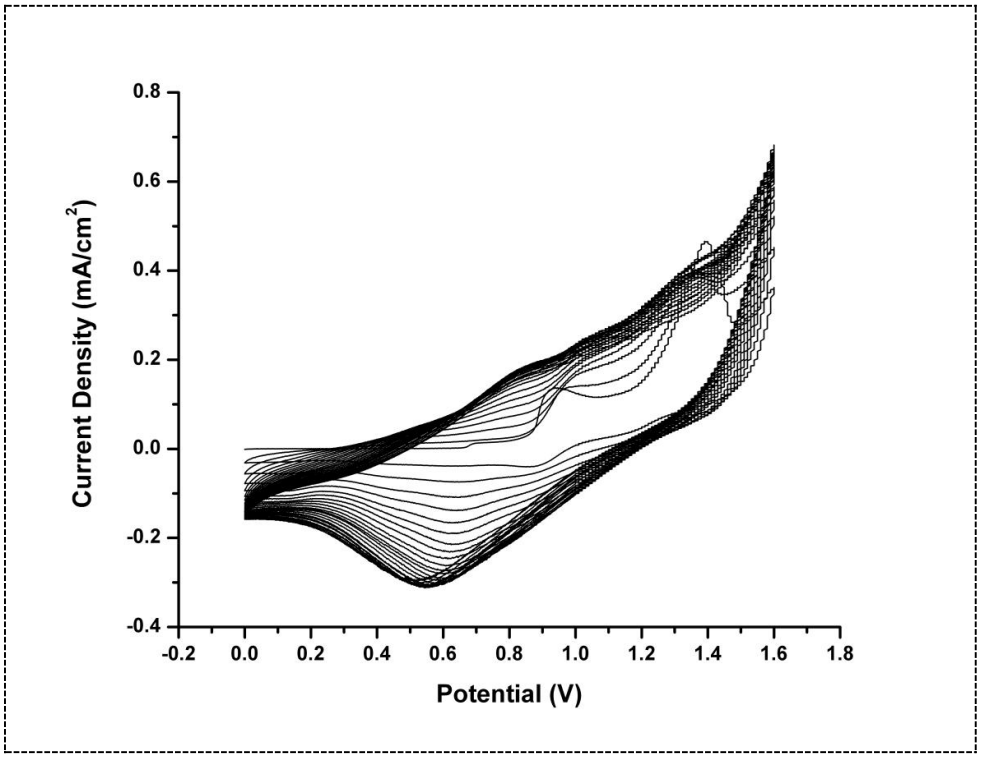

Figure 3.1. Repeated potential scan electropolymerization of **BSeTT** in 0.1M $NaClO_4$/ $LiClO_4$ /ACN:DCM (95:5)After electrochemical polymerization, in order to investigate redox behaviours of the **PBseTT** polymer coated ITO electrodes were subjected to CV in a monomer free 0.1 M $LiClO_4$/$NaClO_4$/ACN solution. As illustrated in Figure 3.2, a reversible p-doping at 1.17 V for **PBSeTT** were recorded.

HOMO and LUMO energy levels of the polymer (**PBSeTT)** were investigated using the onset of the corresponding oxidation potentials (Figure 3.2) against Fc/Fc^+ reference electrode (NHE was taken as 4.75 eV vs. vacuum). HOMO energy level were calculated as -5.88 eV for **PBSeTT.** The corresponding polymer has only p-doping characteristics, so LUMO energy levels were calculated from HOMO and optical band gap values as -4.95 eV.

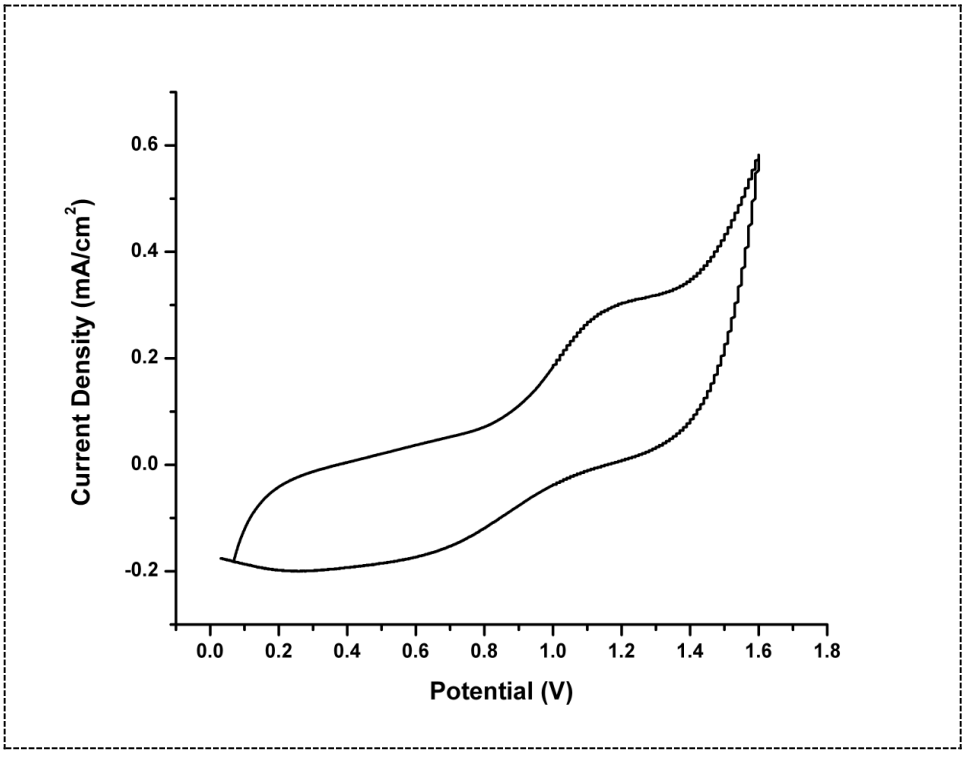

Figure 3.2. Single scan cyclic voltammogram of electrochemically synthesized **PBSeTT** in 0.1 M $LiClO_4$/$NaClO_4$/ACN solution.

The scan rate dependence of doping-dedoping process is important to investigate whether this process is the non-diffusion controlled or not. For this purpose single scan cyclic voltammogram of the polymer film was recorded at different scan rates and the scan rate dependence of **PBSeTT** (Figure 3.3) was investigated.

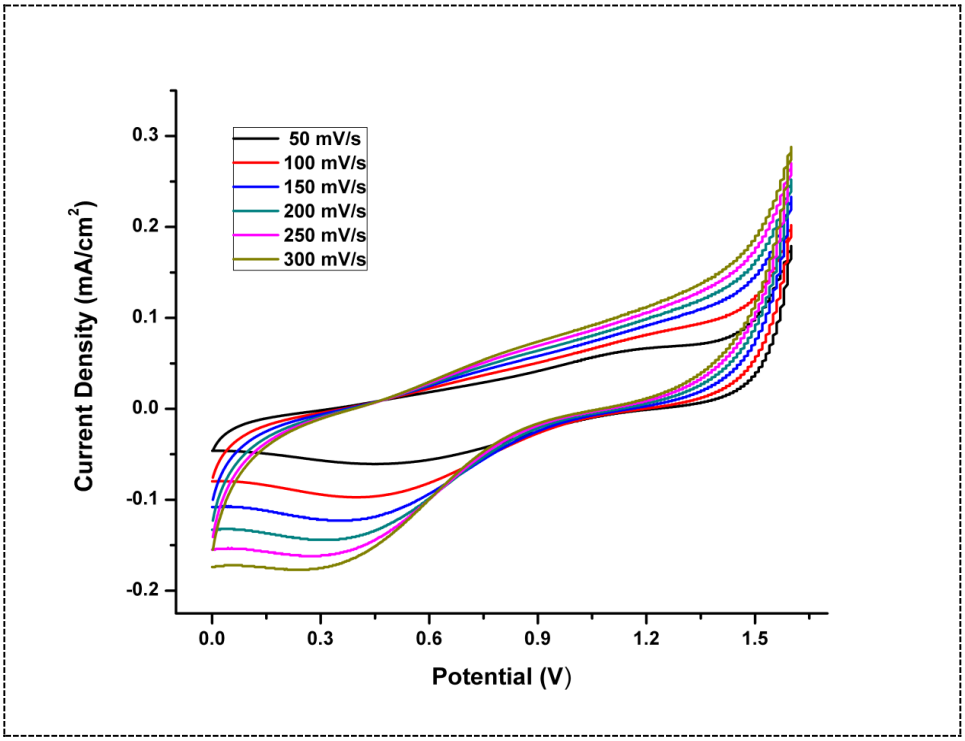

Figure 3.3. Scan rate dependence of **PBSeTT** in a 0.1 M $NaClO_4$–$LiClO_4$/ACN solution at 50, 100, 150, 200, 250, and 300 mV/s

Linear relationship between the current density and the scan rate proves that the electroactive polymer films were well adhered and the redox processes were non-diffusion controlled. (Figure 3.4)

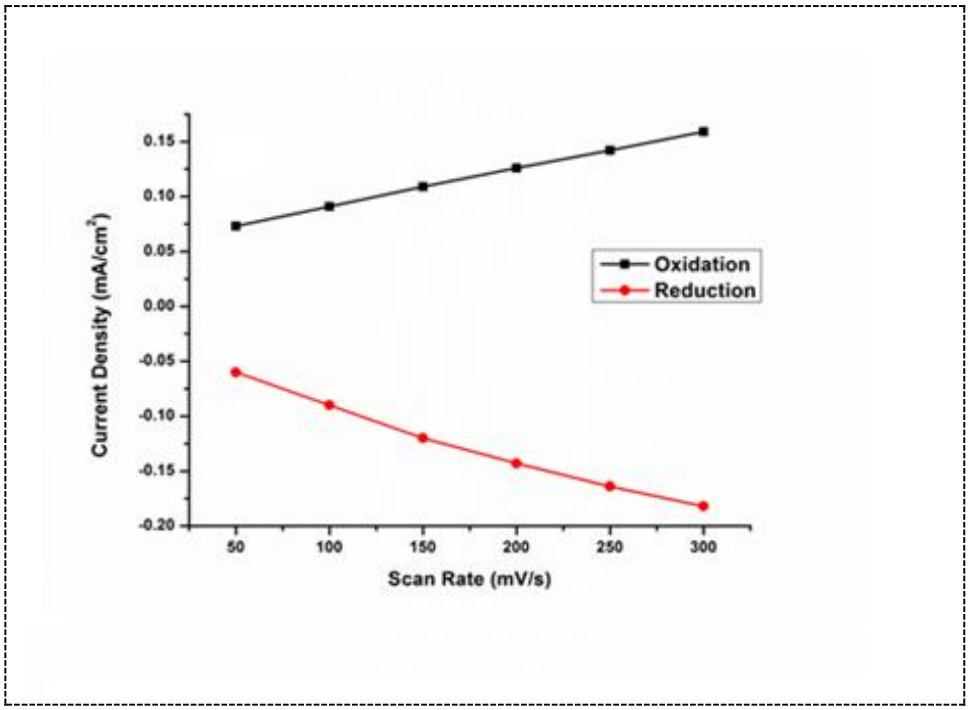

Figure 3.4. Linear relationship between the current density and the scan rate of **PBSeTT**

3.1.1.2 Spectroelectrochemistry Properties of PBSeTT

Spectroelectrochemical studies mainly focus on optical changes and electronic transitions as a results of applied potentials.

3.1.1.2.1 Electronic and Optical Studies of PBSeTT

Electronic and optical studies polymer film was prepared via electrochemically as described before and all these studies conducted into 0.1 M $NaClO_4$–$LiClO_4$/ACN solutions by using UV-Vis-NIR spectrophotometer via incrementally increasing applied potential between 0.0 V and 0.95 V for **PBSeTT**, which were decided from CV results reported in Figure 3.1.

Before performing stepwise oxidation corresponding polymer **(PBSeTT)** was reduced to its neutral states to get a real neutral state absorption and to remove any trapped charge and dopant ion remained from electrochemical polymerization.

Upon stepwise oxidation, while the absorption in the visible region centered at 525 nm for **PBSeTT** started to decrease, new bands were appeared at around 900 nm and 1300 nm due to the formation of charge carriers on the polymer backbone namely polaron (radical cation) and bipolaron (dication) (Figure 3.5). **PBSeTT** revealed one absorption maxima in the visible region.

From spectroelectrochemical studies besides λ_{max} values, optical band gaps of these type of materials could be calculated. Optical band gap (Eg^{op}) of **PBSeTT** film was determined from the lowest energy π-π* transitions (525 nm for **PBSeTT**), and the following value was found as 0.93 eV.

PBSeTT has a wide range of absorption [nearly full visible absorption] in the visible region which makes it dark gray in both states. (Figure 3.6)

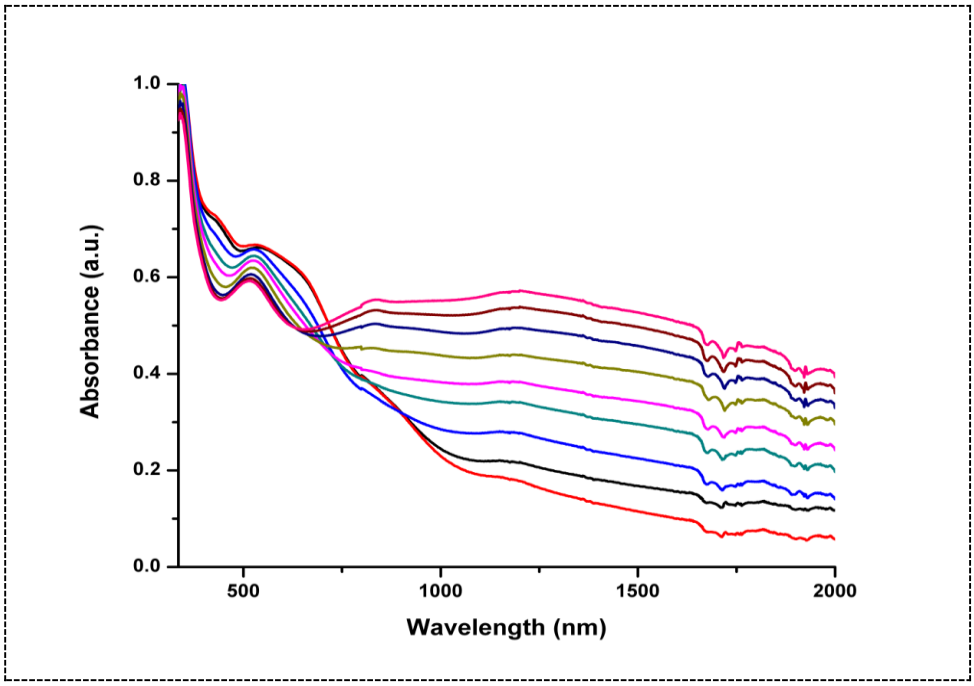

Figure 3.5. Electronic absorption spectra of **PBSeTT** switching between 0.0 V and 0.95 V in 0.1 M $NaClO_4$–$LiClO_4$/ACN solution

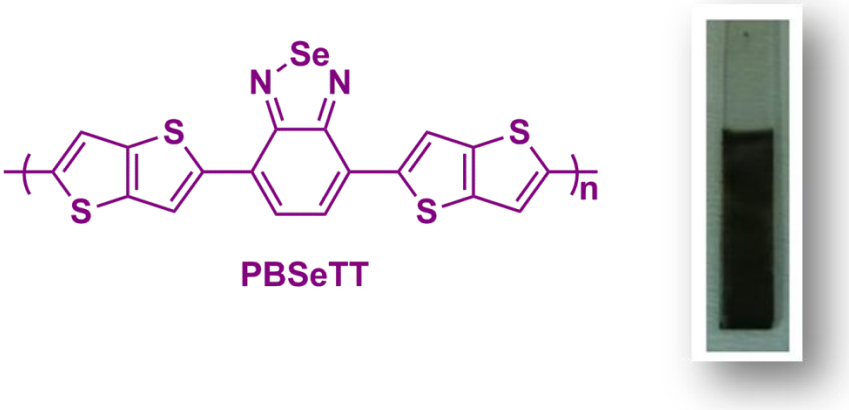

Figure 3.6. Structure and color of **PBSeTT**

3.1.1.3 Kinetic Studies of PBSeTT

Percent transmittance values and switching times for both polymers were monitored in visible and NIR regions by applying square-wave potential steps. Kinetic measurements were performed in a monomer free $NaClO_4$–$LiClO_4$/ACN solvent-electrolyte couple for **PBSeTT.** The specific wavelengths for these scans were determined from the maximum absorbance in the spectrum of the polymer film.

3.1.1.3.1 Electrochromic Contrast And Switching Studies of PBSeTT

PBSeTT revealed 13% optical contrast upon doping/de-doping process with a switching time of 3.1 s in NIR region. Then that showed 4% optical contrast at 525 nm and 13% at 830 nm with 3.1 s and 1.4 s switching times st corresponding wavelengths.

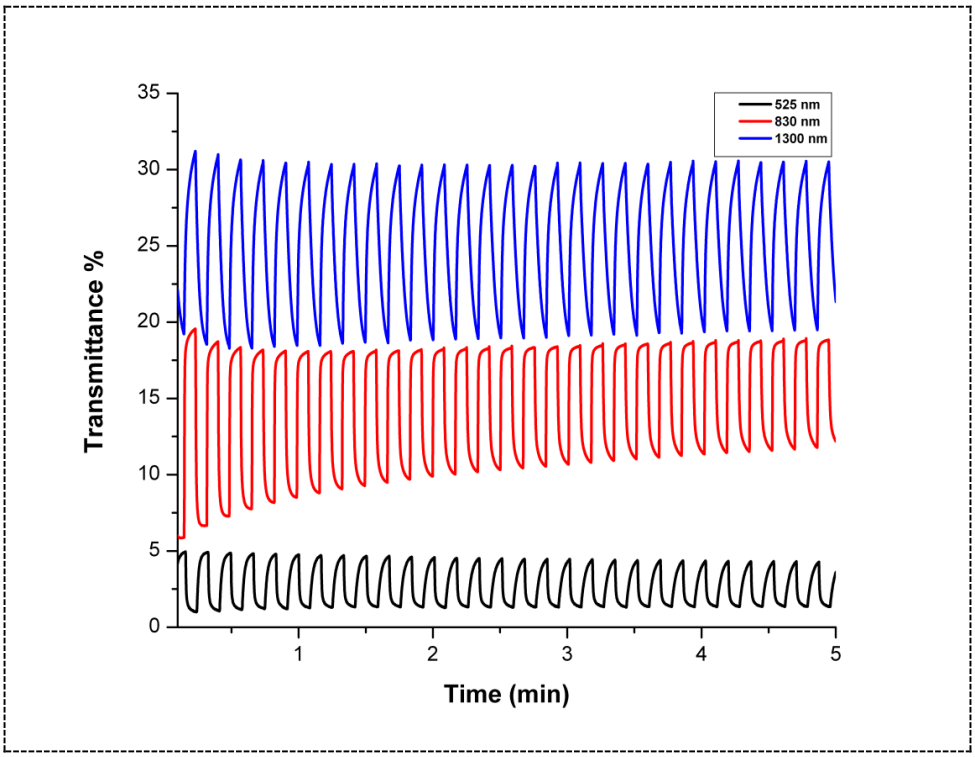

Figure 3.7. Kinetic studies of **PBSeTT** at 525/830/1300 nm

3.1.2 Electrochemical and Electrochromic Properties of PQTT (P2)

3.1.2.1 Electrochemistry of QTT (M2)

QTT were polymerized potentiodynamically on ITO coated glass slide. the system was chosen for electropolymerization of **QTT** as $NaClO_4$/ $LiClO_4$ /ACN:DCM (1:1) solution due to the low solubility of this derivarive. The cyclic voltammograms for electrochemical polymerizations was reported Figure 3.8 which were scanned between 0 V and 1.1V at a scan rate of 100 mV/s.

In the first cycle of CV the irreversible monomer oxidation peak was recorded at 0.83 V for **QTT**. Then, after each successive cycles formation a new reversible redox couple with an increasing current intensity were observed which clarify the formation of electroactive polymer films on ITO surface. (Figure 3.8)

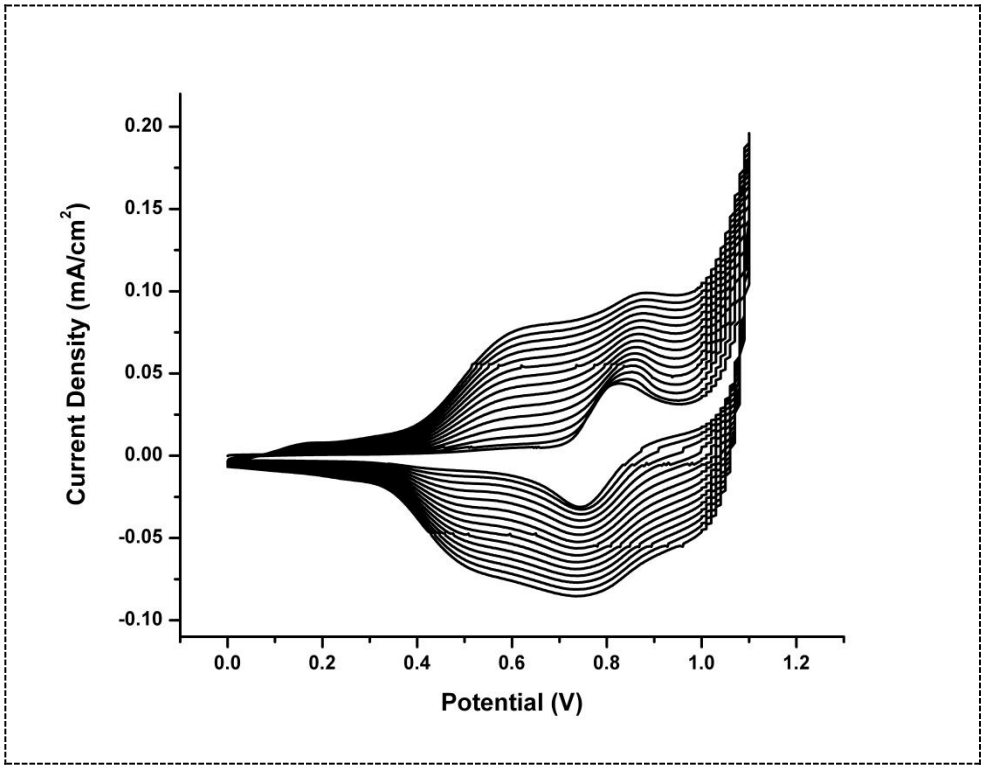

Figure 3.8. Repeated potential scan electropolymerization of **QTT** in 0.1M $NaClO_4$/ $LiClO_4$/ACN:DCM [1:1]

After electrochemical polymerization, in order to investigate redox behaviours of the **QTT** polymer coated ITO electrodes were subjected to CV in a monomer free 0.1 M $LiClO_4$/$NaClO_4$/ACN solution. As illustrated in Figure 3.9, a reversible p-doping at 0.7 V for **QTT** were recorded.

HOMO and LUMO energy levels of the polymer **(PQTT)** were investigated using the onset of the corresponding oxidation potentials [Figure 3.9] against Fc/Fc^+ reference electrode (NHE was taken as 4.75 eV vs. vacuum). HOMO energy level were calculated as -5.47eV for **PQTT.** The corresponding polymer has only p-doping characteristics, so LUMO energy levels were calculated from HOMO and optical band gap values as -4.17 eV.

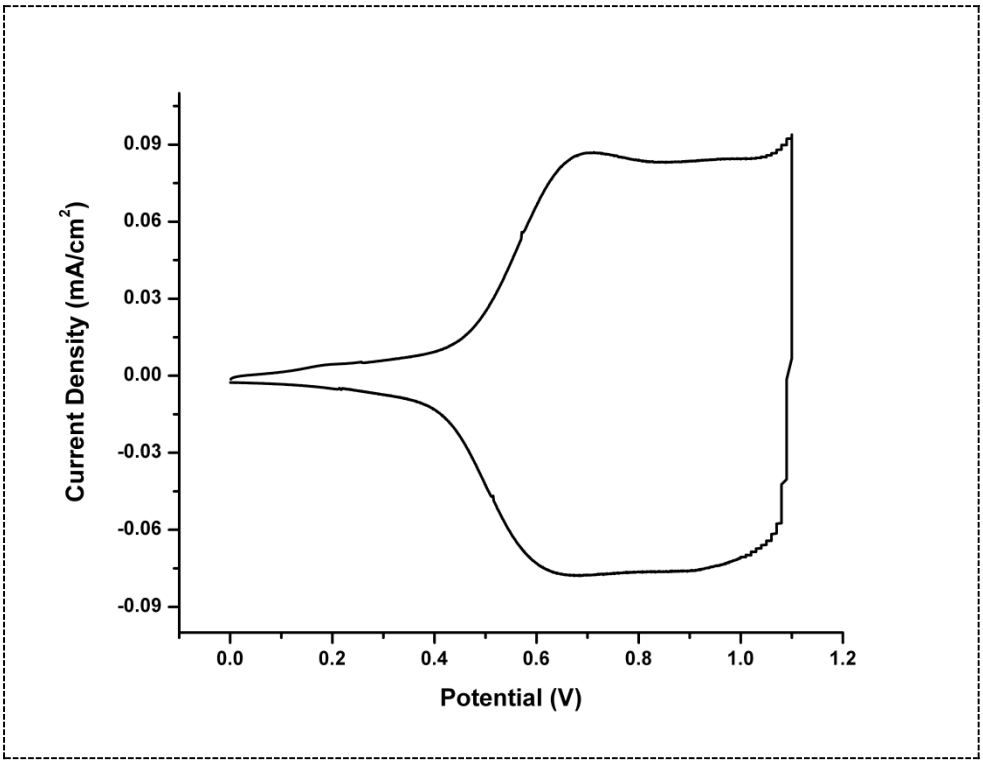

Figure 3.9. Single scan cyclic voltammogram of electrochemically synthesized **PQTT** in 0.1 M $LiClO_4$/$NaClO_4$/ACN solution.

The scan rate dependence of doping-dedoping process is important to investigate whether this process is the non-diffusion controlled or not. For this purpose single scan cyclic voltammogram of the polymer film was recorded at different scan rates and the scan rate dependence of **PQTT** (Figure 3.10) was investigated.

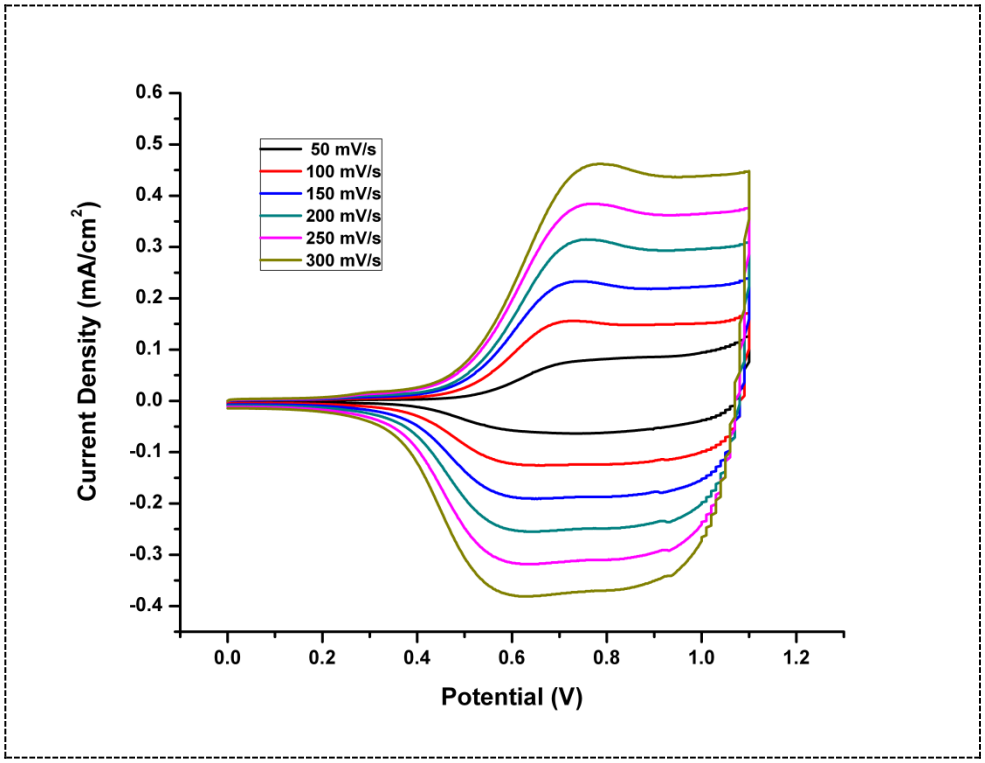

Figure 3.10. Scan rate dependence of **PQTT** in a 0.1 M $NaClO_4$–$LiClO_4$/ACN solution at 50, 100, 150, 200, 250, and 300 mV/s

Linear relationship between the current density and the scan rate proves that the electroactive polymer films were well adhered and the redox processes were non-diffusion controlled. (Figure 3.11)

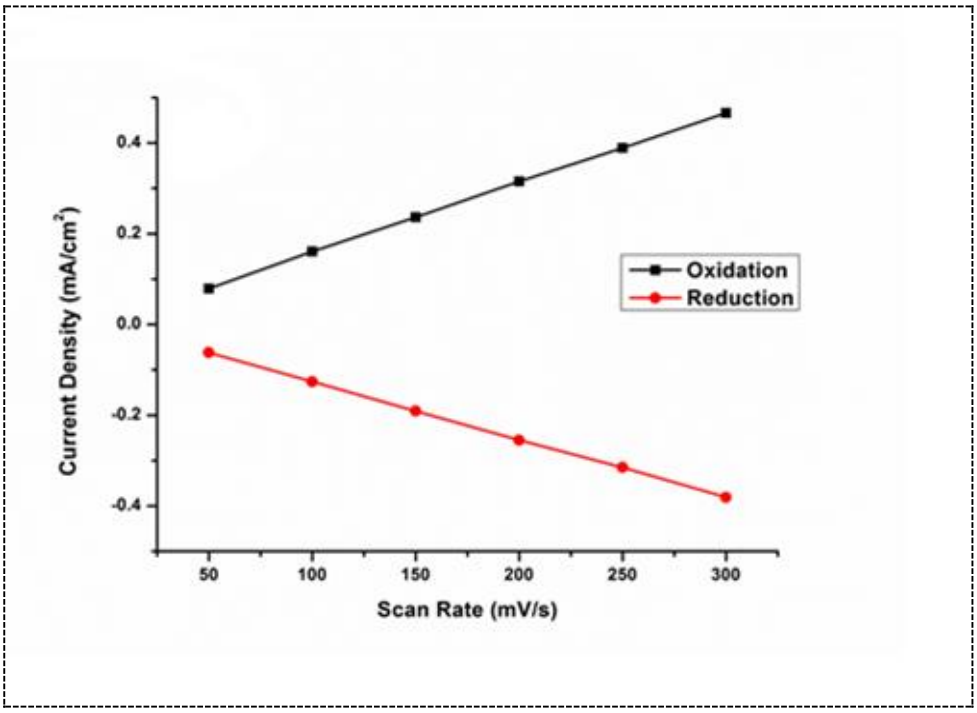

Figure 3.11. Linear relationship between the current density and the scan rate of **PQTT**

3.1.2.2 Spectroelectrochemistry Properties of PQTT

Spectroelectrochemical studies mainly focus on optical changes and electronic transitions as a results of applied potentials.

3.1.2.2.1 Electronic and Optical Studies of PQTT

Electronic and optical studies polymer film was prepared via electrochemically as described before and all these studies conducted into 0.1 M $NaClO_4$–$LiClO_4$/ACN solutions by using UV-Vis-NIR spectrophotometer via incrementally increasing applied potential between 0.0 V and 1.2 V for **PQTT**, which were decided from CV results reported in Figure 3.8.

Before performing stepwise oxidation corresponding polymer [**PQTT**] was reduced to its neutral states to get a real neutral state absorption and to remove any trapped charge and dopant ion remained from electrochemical polymerization.

In the visible region two absorption maxima were recorded for **PQTT** centered at 442 nm and 600 nm. Upon stepwise oxidation, while the absorption in the visible region centered at 600 nm for **PQTT** started to decrease, new bands were appeared at around 800 nm and 1200 nm due to the formation of charge carriers on the polymer backbone namely polaron (radical cation) and bipolaron (dication) (Figure 3.12).

From spectroelectrochemical studies besides λ_{max} values, optical band gaps of these type of materials could be calculated. Optical band gap (Eg^{op}) of **PQTT** film was determined from the lowest energy π-π^* transitions (600 nm for **PQTT**), and the following value was found as 1.30 eV.

PQTT has two absorption peaks in the red and blue regions of the visible spectrum resulted in a neutral state green polymer. After stepwise oxidation, **PQTT** revealed a gray colored oxidized state where almost all visible light was harvested by the polymer film. (Figure 3.13)

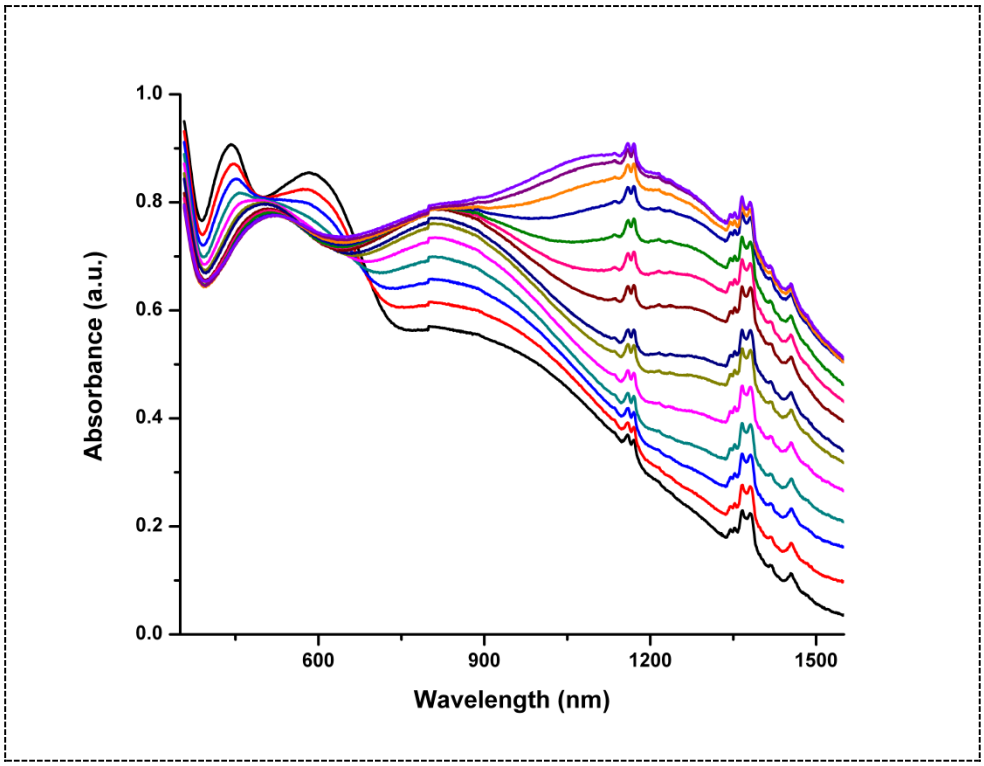

Figure 3.12. Electronic absorption spectra of **PQTT** between0.0 V and 1.2 V in 0.1 M $NaClO_4$–$LiClO_4$/ACN solution

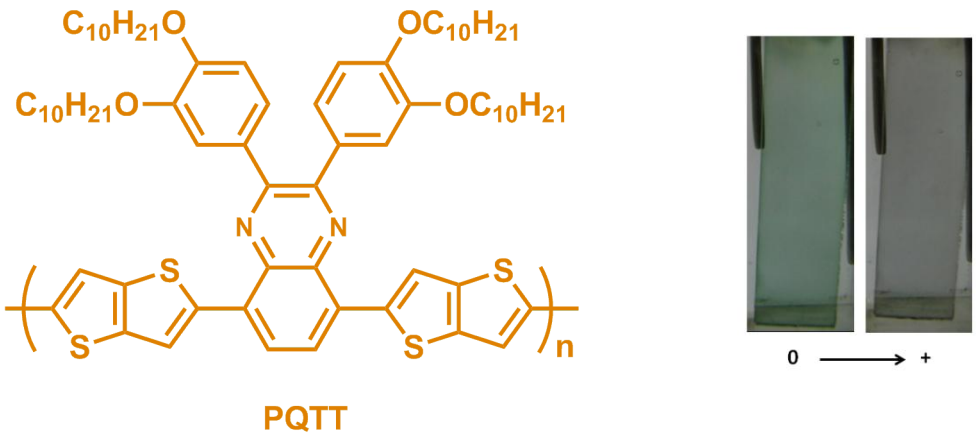

Figure 3.13. Structure and colors of PQTT

3.1.2.3 Kinetic Studies of PQTT

Percent transmittance values and switching times for both polymers were monitored in visible and NIR regions by applying square-wave potential steps. Kinetic measurements were performed in a monomer free $NaClO_4$–$LiClO_4$/ACN solvent-electrolyte couple for **PQTT.** The specific wavelengths for these scans were determined from the maximum absorbance in the spectrum of the polymer film.

3.1.1.3.1 Electrochromic Contrast And Switching Studies of PBSeTT

PQTT revealed 34% optical contrast upon doping/de-doping process with a switching time of 0.5 s in NIR region. Then that showed 13% optical contrast at 440 nm and 12% at 800 nm with 0.3 s and 0.3 s switching times at corresponding wavelengths.

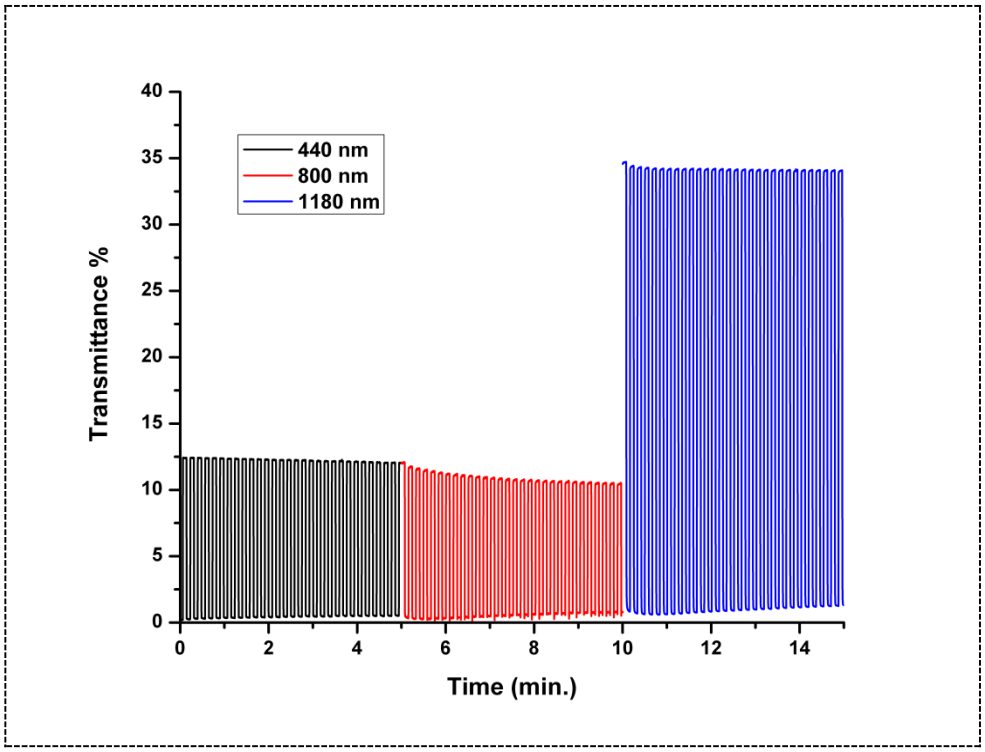

Figure 3.14. Optical contrasts and switching times for **PQTT** recorded at different wavelengths in 0.1 M $NaClO_4$–$LiClO_4$/ACN solution.

Table 3.1. Electrochemical and optical properties of **PBSeTT** and **PQTT**

	HOMO	LUMO[a]	λmax	Eg^{op}
PBSeTT	-5.88 V	-4.95 V	530nm	0.93 eV
PQTT	-5.47 V	-4.17 V	442/600nm	1.30 eV

Table 3.2. Summary of kinetic and optic studies of **PBSeTT** and **PQTT**

Optical Contrast (ΔT%)			Switching Time (s)
PBSeTT	4%	**525 nm**	3.1
	13%	**830 nm**	1.4
	13%	**1300 nm**	3.1
PQTT	13%	**440 nm**	0.3
	12%	**800 nm**	0.3
	34%	**1180 nm**	0.5

CHAPTER 4

CONCLUSION

In this study, two novel donor-acceptor type monomers were synthesized via Stille cross coupling reaction. Both of these materials that have thienothiophene **(TT)** as a donor unit are conducting polymers. While **PBSeTT** contains selenadiazole moiety, **PQTT** includes quinoxaline moiety as an acceptor.

NMR was used for the characterization of corresponding monomers. In order to polymerise these monomers, electropolymerization methodology was performed. Electrochemical, spectroelectrochemical and kinetic properties of these materials were investigated.

PBSeTT and **PQTT** showed p-doping property where a reversible redox couple at 1.17 V and 0.7 V respectively versus Ag wire pseudo reference electrode.

When the shapes of single scan cyclic voltammograms compared, it can be predicted that **PQTT** has more charge trapping capacity than that of **PBSeTT**. In addition, in terms of the oxidation potentials of **PBSeTT** and **PQTT**, the lower oxidation potenatial of **PQTT** can be attributed to the different electron density of acceptor units in the strucutre.

HOMO energy levels of corresponding polymers was obtained as -5.88 eV and -5.47. Due to these polymers (**PBSeTT** and **PQTT**) have only p-dopable characteristics LUMO energy levels were calculated from HOMO and optical band gap values as -4.95 and -4.17, respectively.

Optical band gap values (Eg^{op}) of **PBSeTT** and **PQTT** were calculated from the onset of lowest energy π-π* transitions as 0.93 and 1.30, respectively. Calculated Eg^{op} values state that both polymers can be regarded as low band gap polymers.

Comparison among monomers showed that increasing electron density of donor units decreases the band gap of the monomers where donor acceptor couple is a substantial effect on the electronic properties of donor-acceptor-donor material. **PQTT** has lower oxidation potential and band gap. **PQTT** will be used as active materials in future display technology. Moreover, **PBSeTT** which has broadest absorbtion than others which makes it a good candidate for solar cell applications.

While **PBSeTT** revealed only one absorption maxima in the visible region at 525 nm two absorption maxima were recorded for **PQTT** centered at 442 nm and 600 nm.

PBSeTT showed 4% transmittance at 525 nm, 13% transmittance at 830 nm, and 13% transmittance at 1300 nm. Switching times were obtained as 3.1, 1.4, and 3.1 at coresponding wavelengths.

PQTT demonstrated 34% transmittance at 1180nm, 12% transmittance at 800 nm, 13% transmittance at 440 nm. Switching times were calculated as 0.5, 0.3, and 0.3 s at corresponding wavelengths.

When benzoselenadiazole and quinoxaline based polymers **PBSeTT** and **PQTT** are compared in terms of their electrochromic contrast and switching abilities, it was clearly seen that **PQTT** has shorter switching times and higher percent transmittance values than that of **PBSeTT** which is also consistent with the literature.

REFERENCES

[1] Shirakawa H., Louis E.J., MacDiarmid A.G., Chiang C.K., Heeger A.J., *J.Chem. Soc. Chem. Commun*., **1977**, 578.

[2] Shirakawa H., in Handbook of Conducting Polymers, 2nd ed.; T.A. Skotheim,R.L. Elsenbaumer, J.R. Reynolds, Eds.; Marcel Dekker: New York, **1998**, 197

[3] MacDiarmid A. G., *Angew. Chem. Int. Ed*. 40, **2001**, 2581.

[4] Kaneto K., Yoshino K., Iniushi Y., *Solid State Comm*. 46, **1983**, 389.

[5] MacDiarmid A. G., Chiang J. C., Richter A. F, Epstein A. J., *Synth Met*. 18, **1987**, 285.

[6] Kovacıc P., Kyriakis A., *J. Am. Chem. Soc*. 85, **1963**, 454.

[7] Wnek G.E., Chine J.C., Karasz F.E., Lillya C.P., *Polymer* 20, **1979**, 1441.

[8] Garnier F., Hajlaoui R., Yassar A., Srivastava P., *Science* 265, **1992**, 684.

[9] Halls J.J.M., Walsh C.A., Greenham N.C., Marseglia E.A., Friend R.H., Moratti S.C., Holmes A.B. *Nature* 376, **1995**, 498.

[10] Friend R.H., Gymer R.W., Holmes A.B., Staring E.G.J., Taliani C., Bradley D.DC., dos Santos DE., Bredas J.L., Lögdlund M., Salaneck W.R. *Nature*, 397, **1998,** 121.

[11] Hwang L.S., Ko J.M., Rhee H.W., Kim C.Y., *Synth. Met.* 55, **1993**, 3671.

[12] Bobacka J., *Anal. Chem.* 71, **1999**, 4932.

[13] Maa L. J., Li Y. X., Yu X. F., Yang Q. B., Noh C. H., *Sol. Energy Mater. Sol. Cells* 93, **2009**, 564.

[14] Schwendeman I., Hickman R., Sonmez G., Schottland P., Zong K., Welsh D. M., Reynolds J. R., *Chem. Mater*. 14, **2002**, 3118.

[15] Bredas L., Street G. B., *Acc. Chem. Res.* 18, **1985**, 309.

[16] Hoffmann R., *Angew. Chem. Int. Ed*. 26, **1987**, 846.

[17] Chiang C.K., Fincher C.R., Jr., Park Y.W., Heeger A.J., Shirakawa H., Louis E.J., Gau S.C., and MacDiarmid A.G., *J. Chem. Phys*. **1978,** 69.

[18] MacDiarmid A. G., Heeger A. J., *Synth. Met*., 1, **1979**, 101.

[19] Kanatzidis M. G., *Chem. Eng. News* 68, **1990**, 36.

[20] de Leeuw D. M., Simenon M. M. J.; Brown A. R., Einerhand R. E. F., *Synth. Met.* 87, **1997**, 53.

[21] Mac Diarmid A.G., *Angew. Chem. Int. Ed*. 40, **2001**, 2581.

[22] Duan R. G., PhD thesis, University of Minessota, **1997**.

[23] Toshima N., Hara S., *Prog. Polym. Sci*. 20, **1996**, 155.

[24] Yoshino K., Hayashi R., Sugimoto R., *Jpn. J. Appl. Phys*. 23, **1984**, 899.

[25] Malinauskas A., *Polymer*, 42, **2001**, 3957.

[26] Toshima N., Hara S., *Prog. Polym. Sci*., 20, **1995**, 164.

[27] Groenendaal L. B., Zotti G., Aubert P. H., Waybright S. M., Reynolds J. R. *Adv. Mater*. 15, **2003**, 855.

[28] Mortimer R. J., Dyer A. L., Reynolds J. R., *Displays* 27, **2006**, 2.

[29] Diaz A. F., Martinez A., Kanazawa K. K., Salmon M. M., *J. Electroanal. Chem.* 130, **1981**, 181.

[30] Reynolds J. R., Hsu S. G., Arnott H. J., *J. Polym. Sci Part B Polym. Phys*. 27, **1989**, 2081.

[31] Zotti G., Gumbs R., *Handbook of Organic Conductive Molecules and Polymers, ed. H.S. Nalwa, Editor*. *Wiley, Chichester*, **1997**.

[32] Garnier F., Horowitz G., Peng X., Fichou D., *Adv. Mater*. 2, **1990**, 592.

[33] Burroughes J. H., Bradley D. C. C., Brown A. R., MacKay M. K., Friend R. H., Burn P. L. , *Nature* 347, **1990**, 539.

[34] Scott C. J., *Science* 278, **1997**, 2071.

[35] MacDiarmid A. G., *Synth. Met*. 84, **1997**, 27.

[36] Tourillon G., Garnier F., Garzard M., Dubois J. C., J. *Electroanal. Chem*. 148, **1983**, 299.

[37] Rowley N. M., Mortimer R.J., *Sci. Prog*. 85, **2002**, 243.

[38] Paoli M. A. De, Gazotti A., Braz J., *Chem. Soc.* 13, **2002**, 410.

[39] Tacconi N. R. de , Rajeshwar K., Lezna R. O., *Chem. Mater*. 15, **2003**, 3046.

[40] Witker D., Reynolds J.R., *Macromolecules* 383, **2005**, 763

[41] Wang S., Todd E. K., Birau M., Zhang J., Wan X., Wang Z. Y., *Chem. Mater.* 17, **2005**, 6388.

[42] Argun A., Aubert P.H., Thompson B. C., Schwendeman I., Gaupp C. L., Hwang J., Pinto N. J., Tanner D. B., MacDiarmid A. G., Reynolds J. R., *Chem. Mater.* 16, **2004**, 4401

[43] Wudl F., Kobayashi M., Heeger A. J., *J. Org. Chem.* 49, **1984**, 3382.

[44] Balan A., Ms. Thesis, Middle East Technical University, **2009.**

[45] Thomas C. A., Zong K., Abboud K. A., Steel P. J., Reynolds J. R., *J. Am. Chem. Soc.* 126, **2004**, 16440.

[46] Unlu N., Kaya T. , Sendur M., Cırpan A., *Mac.Mol.Chem*. 18, **2012**, 1885.

[47] Neto B. A. D., Lopes A. S., Ebeling G., Goncalves R. S., Costa V. E. U., Quina F. H., Dupont J., *Tetrahedron* 61, **2005**, 10975.

[48] Tsubata Y., Suzuki T., Hiyashi T., Yamashita Y., *J. Org. Chem*. 57, **1992**, 6749.

[49] Mohr B., Enkelmann V., Wegner G., *J. Org. Chem*. 59, **1994**, 635.

[50] Zhu S. S., Swager T. M., *J. Am. Chem. Soc*. 119, **1997**, 12568.

[51] Bird, C. W.; Chseesman, . W. H.; Sarefield, A., *A. J. Chem. Soc*. **1963**,4767

[52] Gunbas G., Durmus A., Toppare L., *Adv. Funct. Mater*. 18**, 2008**, 2026.

APPENDIX A

NMR DATA

NMR spectra were recoded on a Bruker Spectrospin Avence DPX-400 Spectrometer. Chemical shifts δ were reported in ppm relative to $CHCl_3$ (^{1}H: δ= 7.27), (^{13}C: δ= 77.0) as internal standarts.

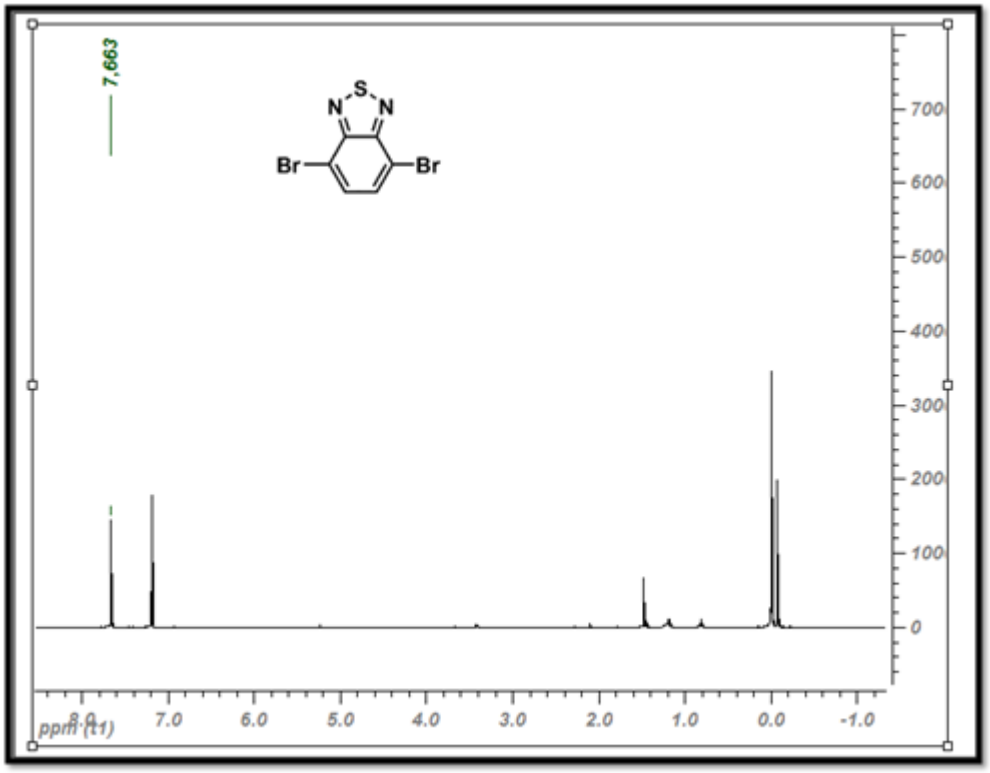

Figure A.1. ^{1}H-NMR data of 4,7-dibromo-2,1,3-benzothiadiazole

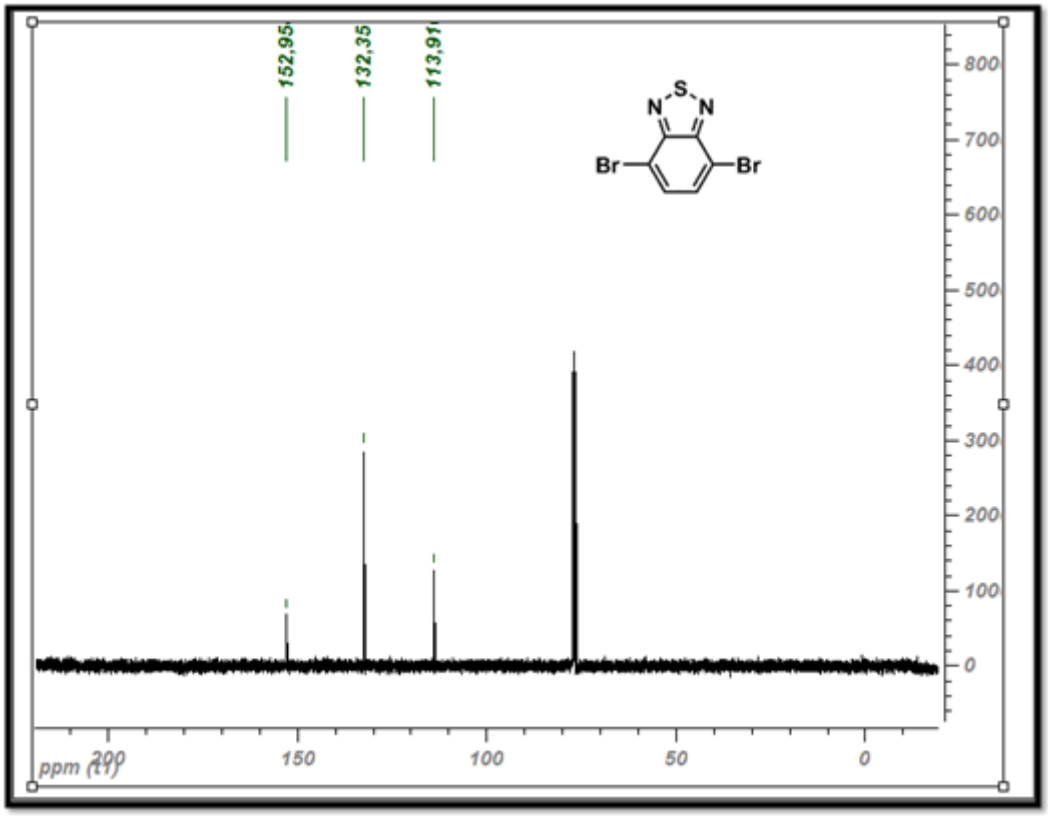

Figure A.2. ^{13}C-NMR data of 4,7-dibromo-2,1,3-benzothiadiazole

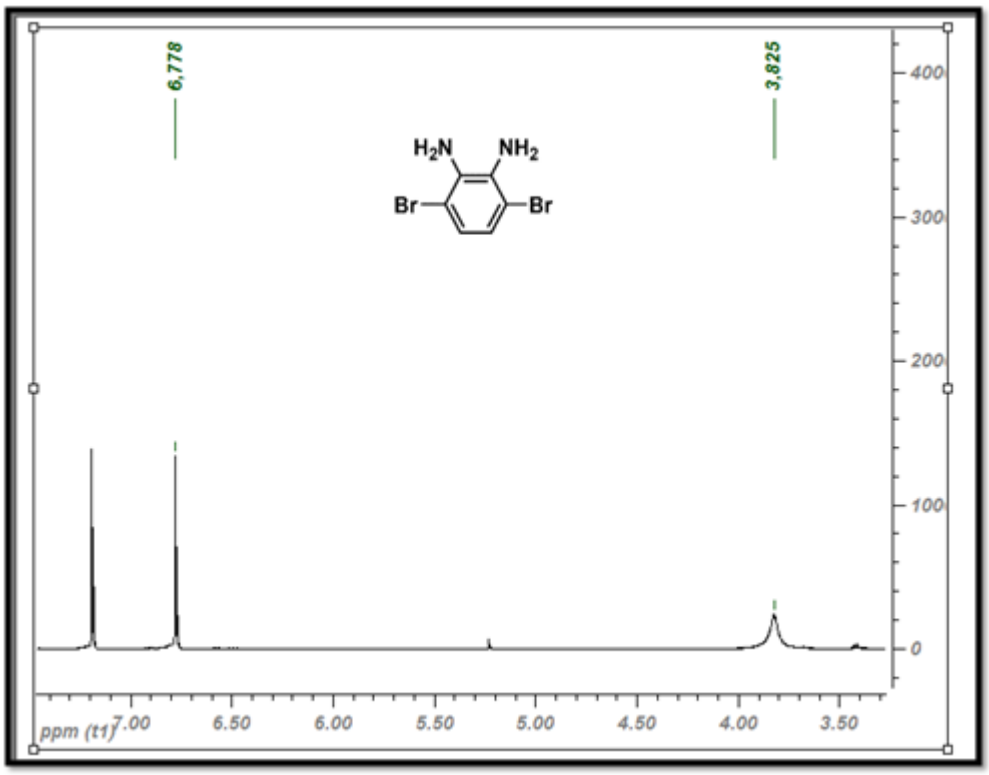

Figure A.3. ^{1}H-NMR data of 3,6-dibromobenzene-1,2-diamine

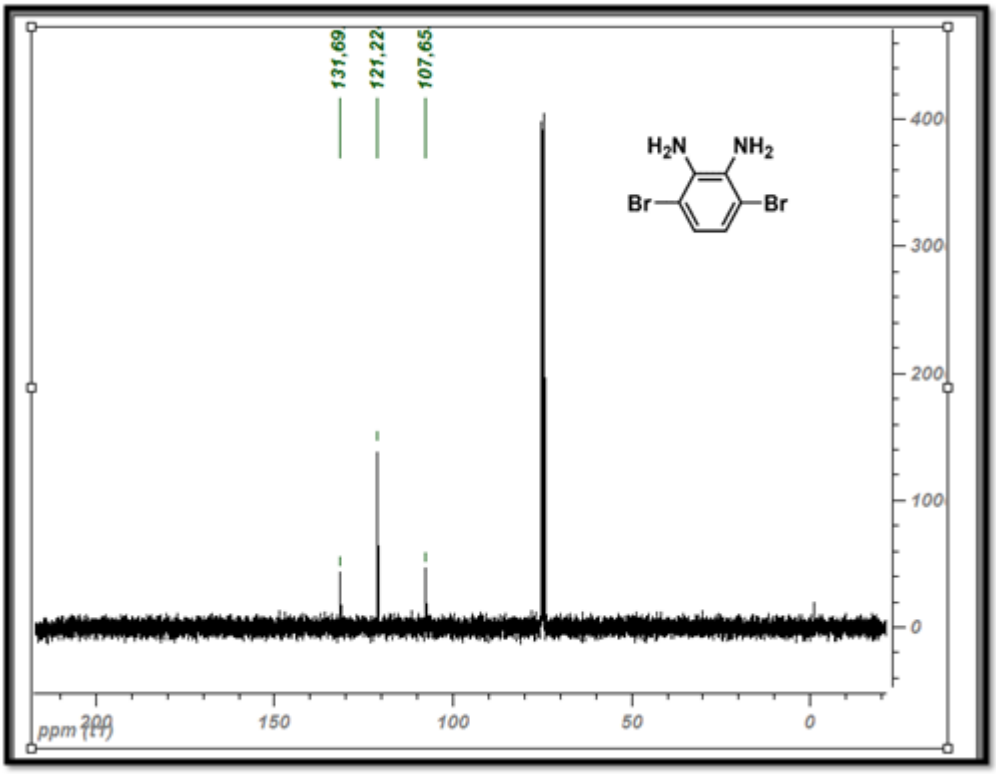

Figure A.4. ^{13}C-NMR data of 3,6-dibromobenzene-1,2-diamine

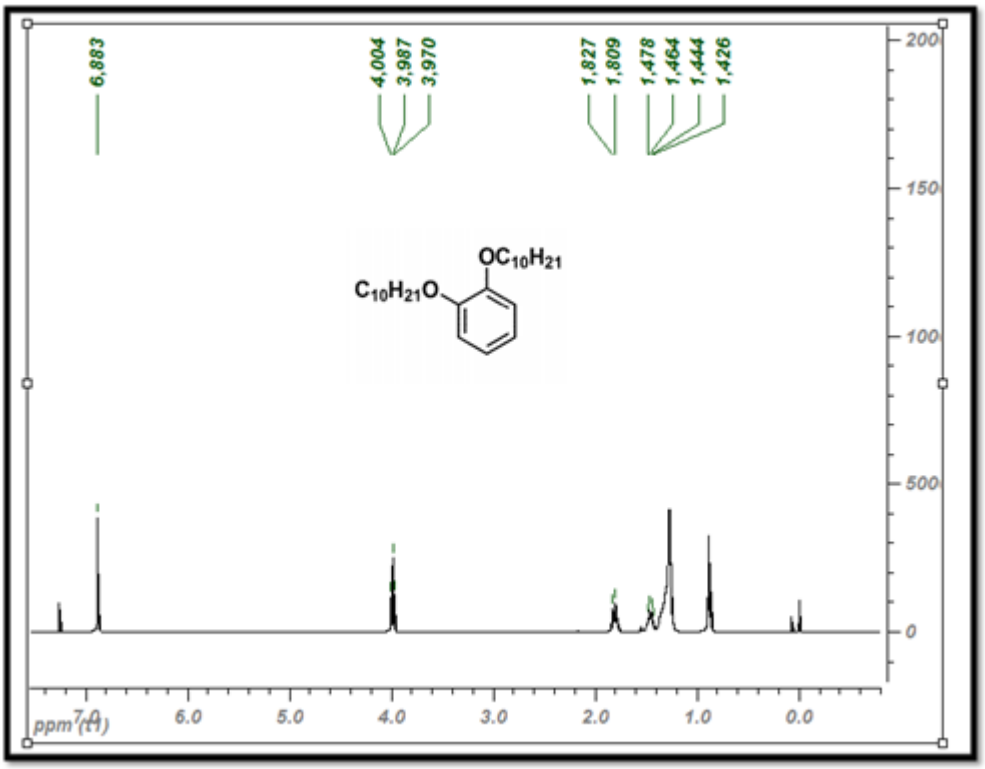

Figure A.5. ^{1}H-NMR data of 1,2-bis[decyloxy]benzene

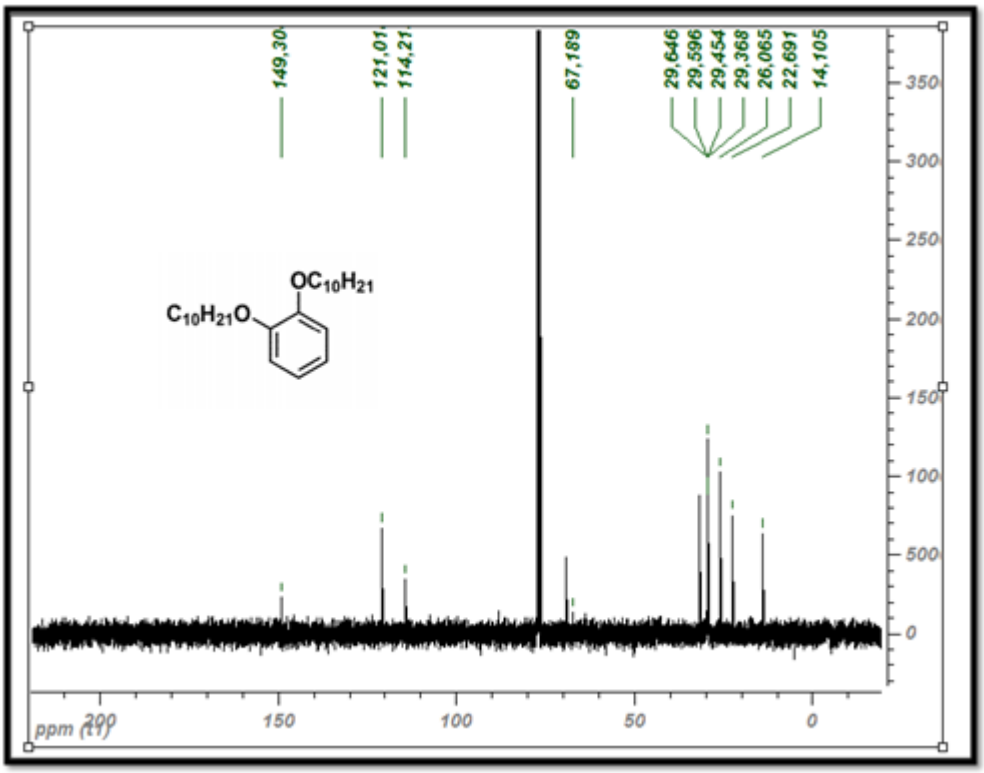

Figure A.6. ^{13}C-NMR data of 1,2-bis[decyloxy]benzene

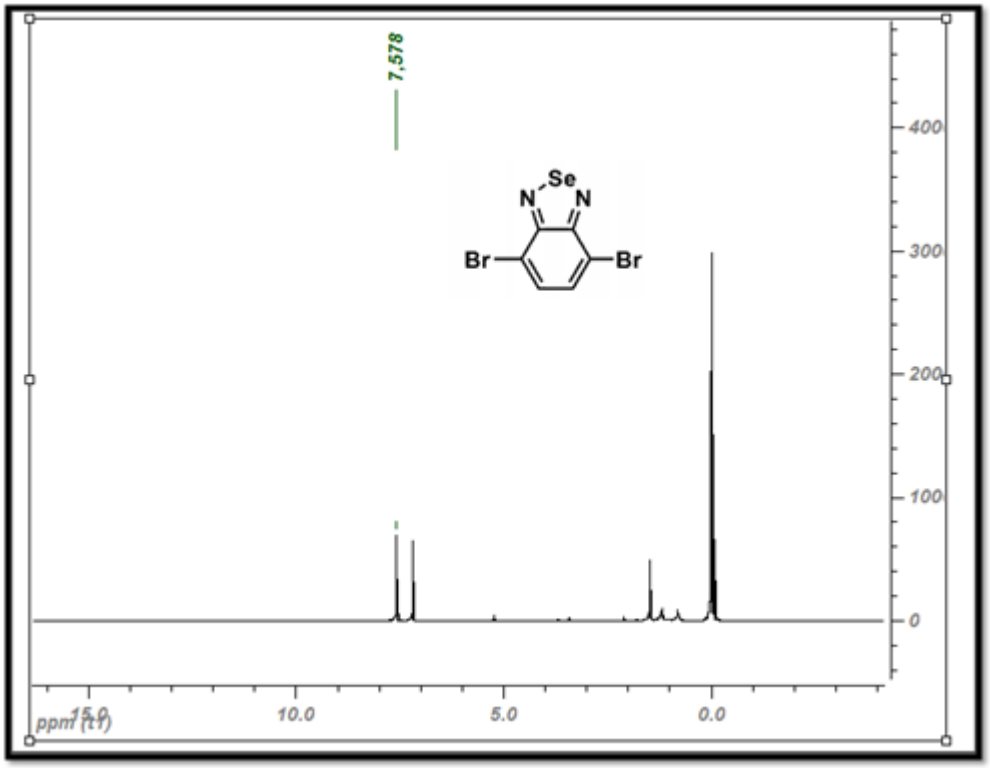

Figure A.7. ^{1}H-NMR data of 4,7-dibromobenzo[c][1,2,5]selenadiazole

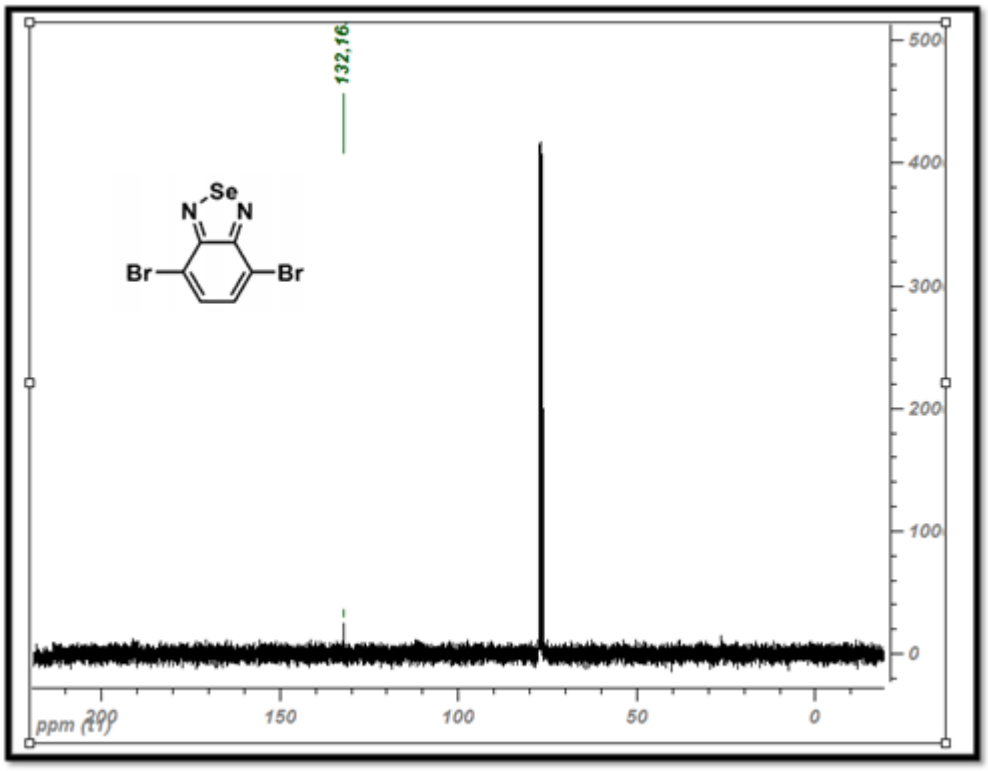

Figure A.8. ^{13}C-NMR data of 4,7-dibromobenzo[c][1,2,5]selenadiazole

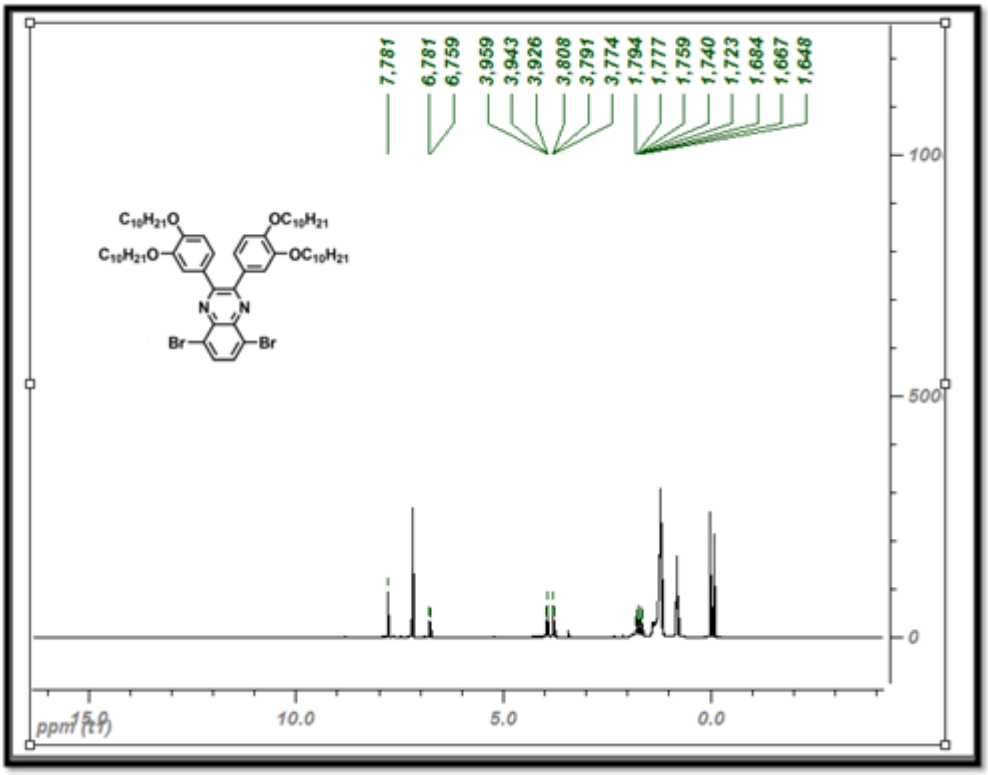

Figure A.9. ^{1}H-NMR data of 2,3-bis[3,4-bis[decyloxy]phenyl]-5,8-dibromoquinoxaline

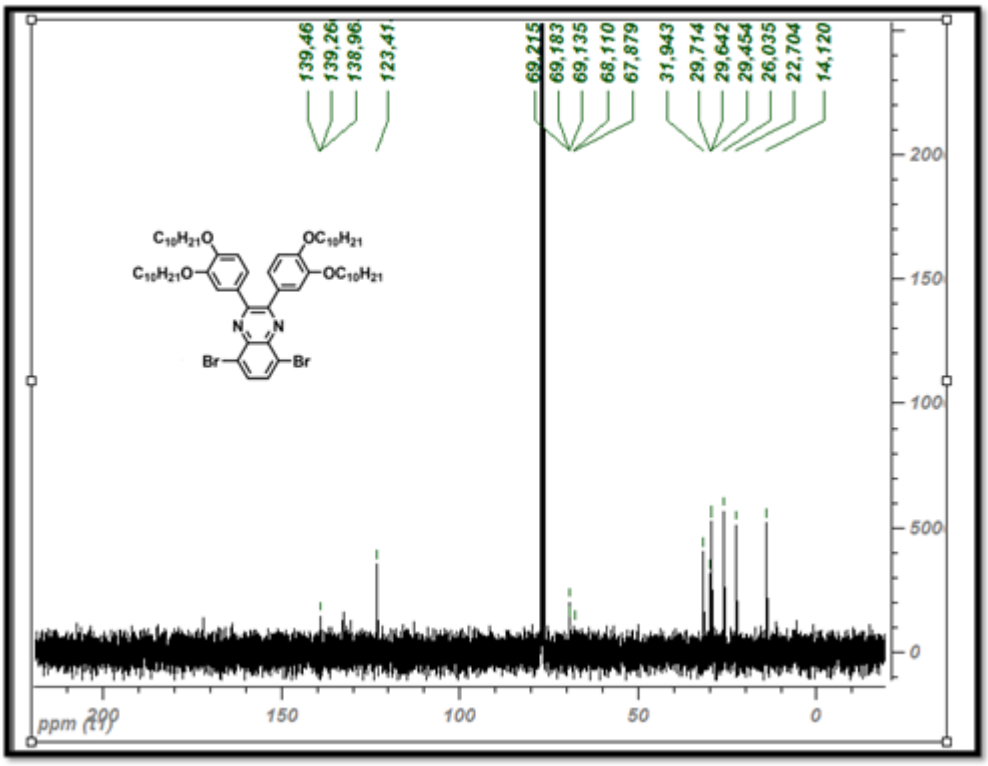

Figure A.10. ^{13}C-NMR data of 2,3-bis[3,4-bis[decyloxy]phenyl]-5,8-dibromoquinoxaline

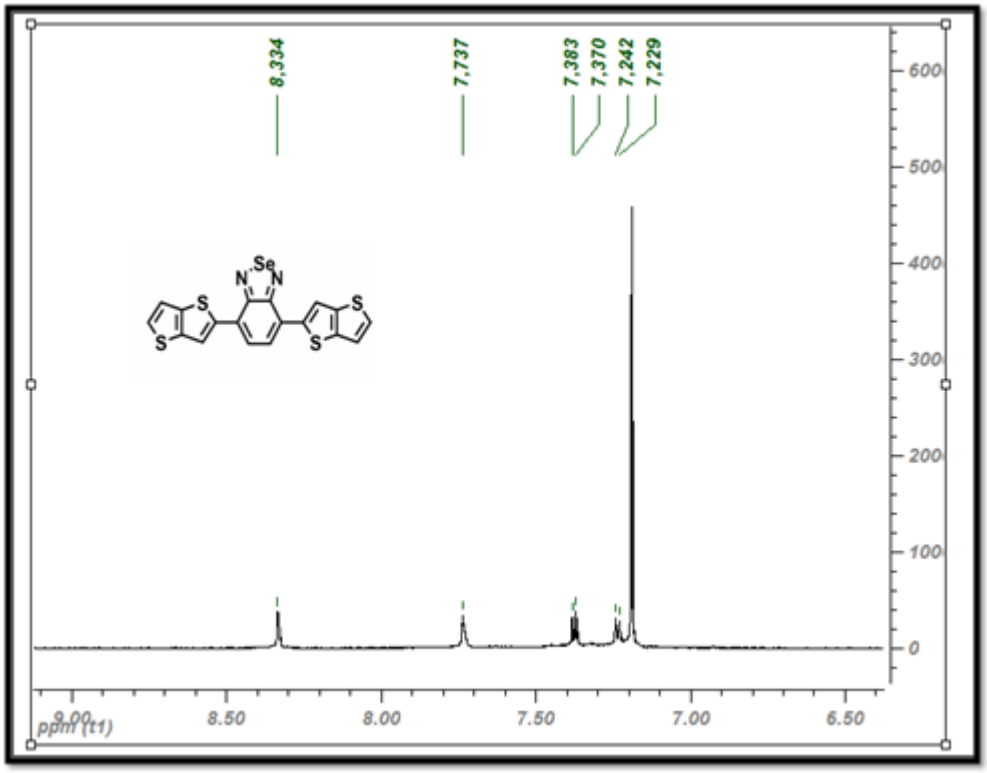

Figure A.11. ^{1}H-NMR data of 4,7-di[thieno[3,2-b]thiophen-2-yl]benzo[c][1,2,5]selenadiazole

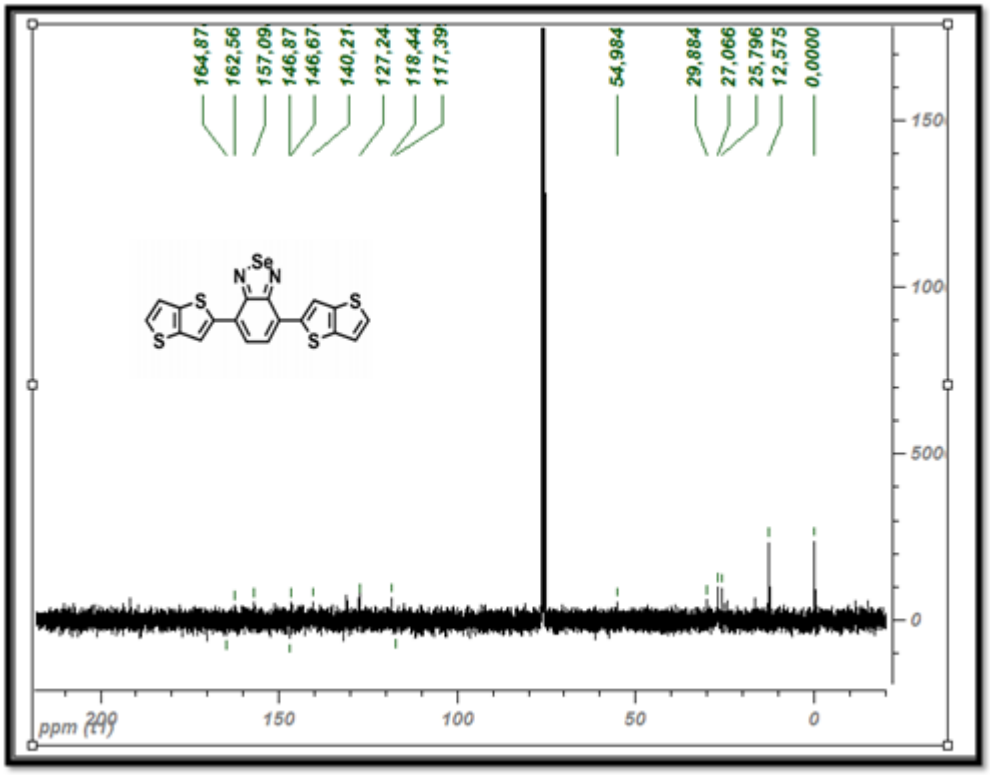

Figure A.12. ^{13}C-NMR data of 4,7-di[thieno[3,2-b]thiophen-2-yl]benzo[c][1,2,5]selenadiazole

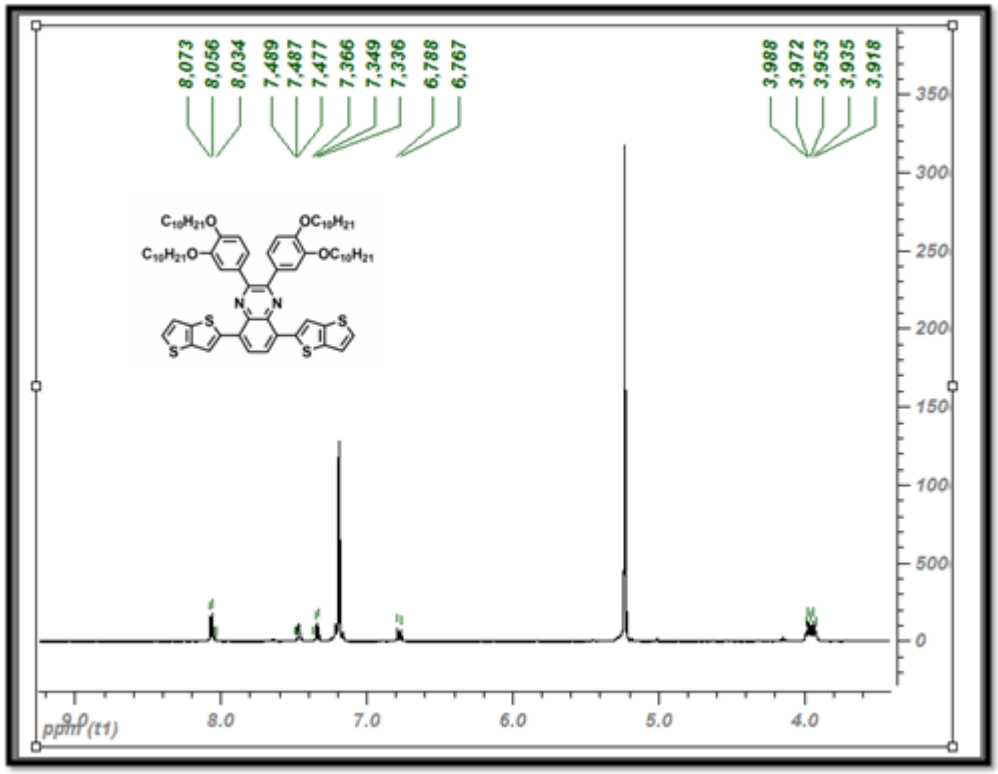

Figure A.13. ^{1}H-NMR data of 2,3-bis[3,4-bis[decyloxy]phenyl]-5,8-di[thieno[3,2-b]thiophen-2-yl]-2,3-dihydroquinoxaline

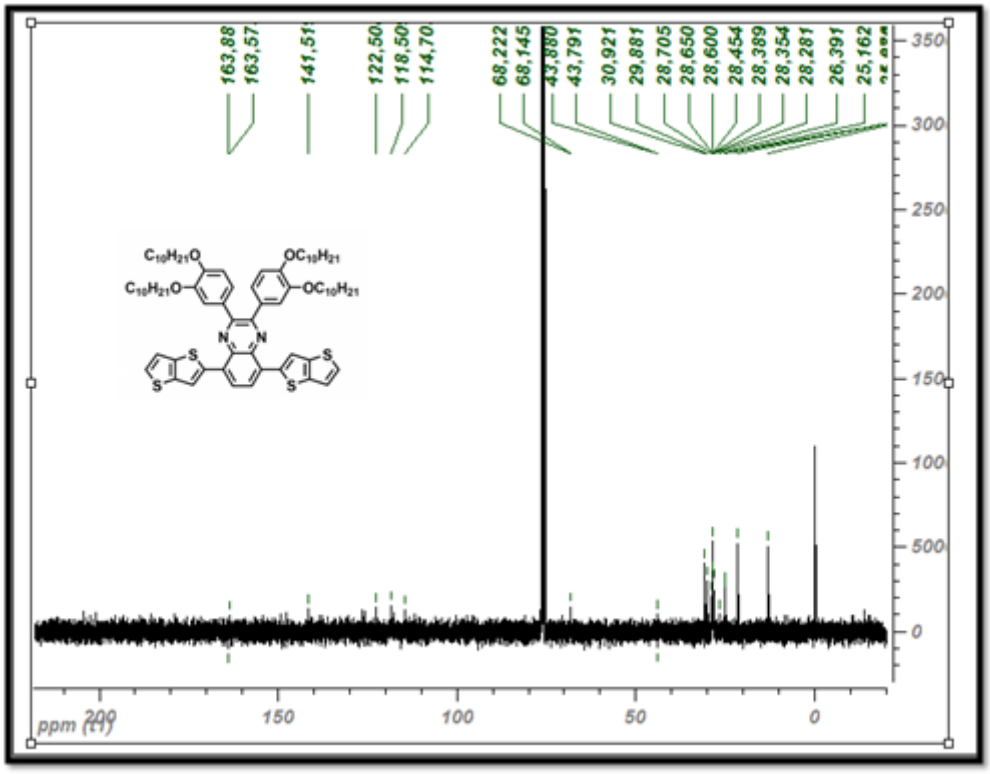

Figure A.15. ^{13}C-NMR data of 2,3-bis[3,4-bis[decyloxy]phenyl]-5,8-di[thieno[3,2-b]thiophen-2-yl]-2,3-dihydroquinoxaline